Chemical, thermal and mechanical stabilities of metal–organic frameworks

Ashlee J. Howarth[1], Yangyang Liu[1]*, Peng Li[1], Zhanyong Li[1], Timothy C. Wang[1], Joseph T. Hupp[1] and Omar K. Farha[1,2]*

Abstract | The construction of thousands of well-defined, porous, metal–organic framework (MOF) structures, spanning a broad range of topologies and an even broader range of pore sizes and chemical functionalities, has fuelled the exploration of many applications. Accompanying this applied focus has been a recognition of the need to engender MOFs with mechanical, thermal and/or chemical stability. Chemical stability in acidic, basic and neutral aqueous solutions is important. Advances over recent years have made it possible to design MOFs that possess different combinations of mechanical, thermal and chemical stability. Here, we review these advances and the associated design principles and synthesis strategies. We focus on how these advances may render MOFs effective as heterogeneous catalysts, both in chemically harsh condensed phases and in thermally challenging conditions relevant to gas-phase reactions. Finally, we briefly discuss future directions of study for the production of highly stable MOFs.

Metal–organic frameworks (MOFs) are a scientifically compelling and functionally evolving class of meso-, micro- and ultramicroporous materials[1–9]. MOF structures encompass dozens of topologies[10], including several, such as sodalite and Rho, that are also well known for zeolites. MOFs are composed of metal nodes and organic linkers (BOX 1) that can be systematically tuned in terms of chemical composition and precise arrangement — an attribute that differs from purely inorganic zeolites, which consist largely of silicon or aluminium ions linked by oxygen atoms. This fine control over the inorganic and organic components of MOFs offers an exceptionally large set of synthetically accessible and remarkable structures, including the possibility of designing functional MOFs that result in various chemical behaviours. Using this approach, crystalline MOFs with large and permanent molecular-scale porosity (up to 90% free volume), ultrahigh surface areas (up to 7,000 $m^2 g^{-1}$) and low densities (down to 0.13 $g cm^{-3}$) have been obtained[11–14]. As a consequence of these properties, MOFs have been explored for many applications including, but not limited to, gas storage and release[15–17], chemical separations[18], drug delivery[19], catalysis[20], light harvesting and energy conversion[21,22], and, recently, the degradation of toxic substances such as chemical warfare agents[21,23–26].

The chemical, thermal, hydrothermal and mechanical stabilities of MOFs have been typically perceived as problematic, especially when compared to industrially relevant zeolites, but this is an increasingly dated perception[27–35]. In recent years, the number and diversity of MOF structures have grown significantly, and many water-stable and thermally stable MOFs now exist, enabling an exciting expansion of their application. In addition, the highly crystalline nature of MOFs allows for atomically precise structural characterization and for the use of computational chemistry to predict properties of frameworks that have not been synthesized yet[36–38]. The computational prediction of properties, based on structure, is also an area of active interest for zeolites[39]. Both the synthesis and computational developments enhance the tunability and diversity that is possible for the rational design of MOFs.

Depending on the application envisaged, different functional stabilities are important. For example, chemical (more specifically, hydrolytic) and thermal stabilities are important for industrial uses including gas separation[15], ion exchange[40], water desalination[41] and moderate-temperature heat storage[42,43], as well as many catalytic processes for which high temperatures, varying pH or the presence of water vapour are common[20]. Mechanical stability has a crucial role if compacted forms of MOFs, such as pellets, are required in industrial processes[44].

Also of considerable interest, but not discussed in this Review, are MOF design principles and stability challenges related to hydrous (<100 °C) and an hydrous (>100 °C) proton transport under harsh acidic

[1]*Department of Chemistry, Northwestern University, 2145 Sheridan Road, Evanston, Illinois 60208–3113, USA.*
[2]*Department of Chemistry, Faculty of Science, King Abdulaziz University, Jeddah, Saudi Arabia.*
**These authors contributed equally to this work.*
Correspondence to O.K.F. and J.T.H.
o-farha@northwestern.edu; j-hupp@northwestern.edu

Article number: 15018
doi:10.1038/natrevmats.2015.18
Published online 9 Feb 2016

conditions in hydrogen fuel cells[45–47], the separation of corrosive acidic gases (for example, H_2S) from volatile hydrocarbons[48], the capture of chemical threats such as ammonia[48,49], and the controlled release of MOF–particle-encapsulated drugs *in vivo*[50–52]. For drug delivery applications, it is essential that instability can be predicted.

Stability of metal–organic frameworks

Although many types of stability are relevant for MOF applications, for simplicity, this Review discusses methods of assessing and imparting chemical, thermal, hydrothermal and mechanical stabilities. In particular, there is a focus on chemical stability in catalysis.

For the purposes of this Review, stability is defined as resistance of the structure to degradation. However, another possible definition is thermodynamic in origin: many functionally stable MOFs (as well as zeolites) are thermodynamically unstable with respect to alternative — typically, denser — polymorphs[53]. An active area of MOF research is the development of routes to thermodynamically unstable, but functionally stable, polymorphs.

Chemical stability. The greatest concerns for the improvement of MOF chemical stability have been largely related to liquid water and water vapour; accordingly, we focus on aqueous solutions[28]. In most MOF

Box 1 | **Metal–organic frameworks**

Metal–organic frameworks (MOFs) are hybrid, crystalline, porous materials made from metal–ligand networks that, in principle, extend infinitely. The inorganic nodes or vertices in the framework consist of metal ions (for example, Cr(III), Fe(III), Al(III), Mn(II), Co(II), Cu(II), Cu(I), Zn(II) and Zr(IV)) or clusters, namely secondary building units (SBUs) (for example, $Zn_4O(COO)_6$, $Cu_2(COO)_4$, $Cr_3O(H_2O)_3(COO)_6$ and $Zr_6O_4(OH)_{10}(H_2O)_6(COO)_6$). Note that by convention, carboxylates (or other linker terminal groups or atoms) are often represented as components of the nodes; see below. These nodes are connected by coordination bonds to organic linkers, which commonly contain carboxylate, phosphonate, pyridyl, and imidazolate or other azolate functional groups. The incorporated organic linkers can be, but are not limited to, bi-, tri- or tetratopic forms. Diverse linkers combined with metal nodes or SBUs possessing different geometries and connectivities give rise to a wide range of framework topologies[10]. In particular, SBUs that define or encompass structural nodes and consist of metal ions plus non-metals (typically, oxygen or nitrogen) provide complementary diversity — especially in terms of topology, connectivity and function. Notably, experimentally realized SBUs now include (collectively) most transition metals, several main-group metals, alkali metals, alkaline earth metals, lanthanides and actinides. The number of metal atoms in these units varies from one to eight or more. The combination of ease of tunability, atomic-level structural uniformity, compositional (elemental) variety and high porosity is, in large measure, what distinguishes MOFs from other porous materials such as activated carbon, porous organic polymers and zeolites.

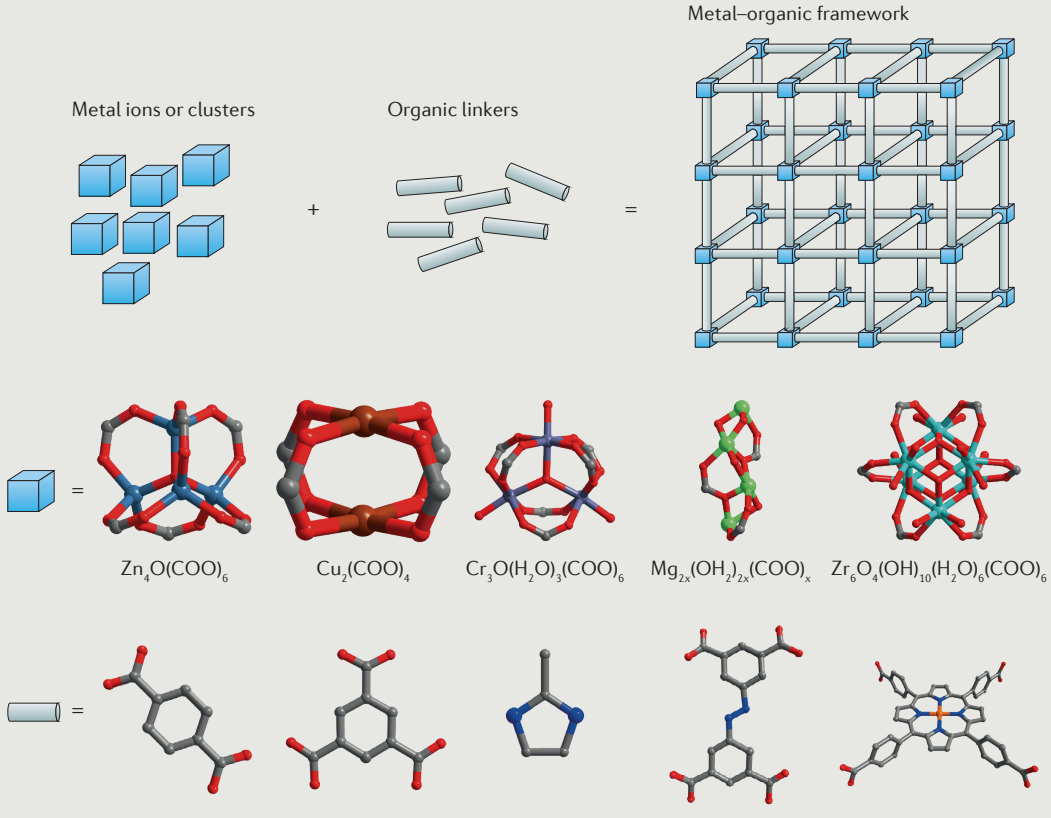

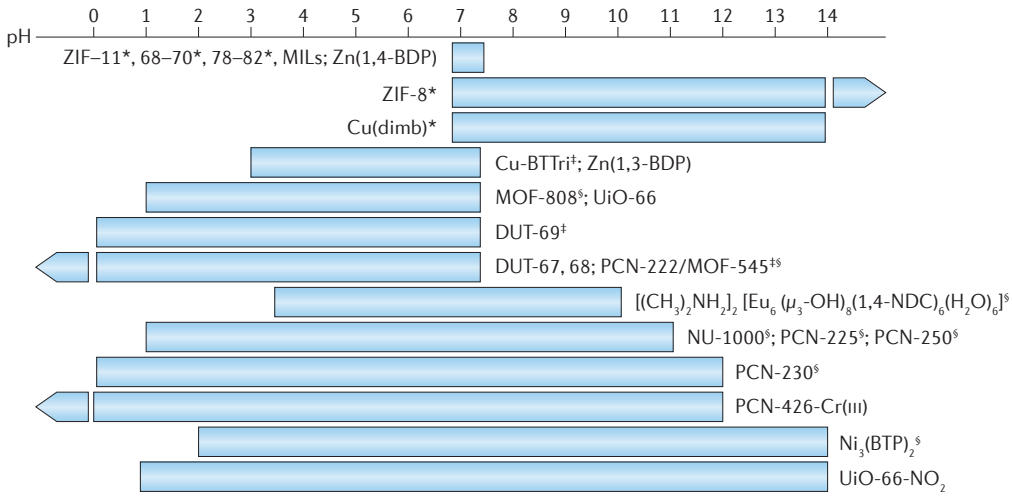

Figure 1 | **The chemical (acid–base) stability of some representative metal–organic frameworks based on literature data.** The bar length indicates the pH range that the metal–organic frameworks (MOFs) can tolerate. An arrow indicates that the MOF can withstand pH < 0 or pH > 14. Stabilities are established by powder X-ray diffraction (PXRD) apart from those marked with '§' (stability confirmed by both PXRD and gas sorption experiments). Studies of stability in aqueous base (†) or aqueous acid (*) have yet to be reported. 1,3-BDP, 1,3-benzenedipyrozolate; 1,4-BDP, 1,4-benzenedipyrozolate; 1,4-NDC, 1,4-naphthalenedicarboxylate; BTP, 1,3,5-tris(1*H*-pyrazol-4-yl)benzene; BTTri, 1,3,5-tris(1*H*-1,2,3-triazol-5-yl) benzene; dimb, 1,4-bis(1*H*-imidazol-4-yl)benzene; DUT, Dresden University of Technology; MIL, Materials Institute Lavoisier; NU, Northwestern University; PCN, porous coordination network; ZIF, zeolitic imidazolate framework.

structures, the chemical weak points are at the nodes — more specifically, the metal–linker bonds — with hydrolysis yielding a protonated linker and a hydroxide (or water) ligated node. Acidic solutions can accelerate the formation of the former, and basic solutions can accelerate the formation of the latter.

Although there is no standard method for assessing the stability of MOFs in acidic, basic or neutral solutions, it is often judged by comparing the powder X-ray diffraction (PXRD) pattern of a MOF before and after soaking it in a given aqueous solution. However, there are no agreed standards for the soaking time or the solution temperature and, as a consequence, making comparisons between different studies is problematic. If the patterns are a close enough match, stability towards the challenge solution is often assumed. Unfortunately, a material that has partially degraded may still pass this test. An instructive secondary test is sorption of an inert gas, construction of an isotherm and, from the isotherm, estimation of the MOF surface area. Loss of MOF surface area, with qualitative retention of the initial PXRD pattern, is typically indicative of partial pore collapse and amorphization. Using these assessment methods, the pH-dependent ranges of aqueous chemical stability of some representative MOFs are summarized in FIG. 1. MOFs labelled with a '§' have been assessed by both PXRD and gas sorption techniques. Not all examples have been tested from pH 0 to 14, and some have shown stability extending below pH 0 or above pH 14 (see FIG. 1 caption to identify such cases). It should be noted that apart from hydroxide ions, only poorly coordinating acids and bases have been used extensively to assess stability. The stability of many MOFs in the presence of strongly coordinating ions (for example, phosphate anions, PO_4^{3-}) has not been observed[54,55]. Contact with strongly coordinating, and potentially MOF-destabilizing, anions can be routinely expected in biological fluids. Recently, a zirconium-based MOF comprising 1,2,3-trioxobenzene linkers was shown to be stable in a phosphate buffer solution at pH 7.4. This may be attributed to the strength of Zr(IV)–trioxobenzene bonds or the absence of μ_3-oxo and -hydroxo bridging moieties in the Zr(IV) nodes of the framework, which may serve as a weak point towards coordinating anions in other zirconium-based MOFs[56].

The use of anionic, nitrogen-containing linkers often yields MOFs that are stable in water; these include zeolitic imidazolate frameworks (ZIFs), other metal–azolate (such as, pyrazolate, triazolate and tetrazolate) frameworks (the term MAF is also used for a class of compounds that includes ZIFs[57]), and 'zeolite-like MOFs' (ZMOFs) that combine azolate and carboxylate coordination capabilities on a single linker[5,30,58–67]. ZIF-8 (FIG. 2a) is a compelling example because it withstands prolonged soaking in 8 M aqueous NaOH at 100 °C. This outstanding hydrolytic stability is attributed, in part, to the hydrophobic nature of the pore openings (namely, apertures). The apertures of ZIF-8 lack polar groups and are too small to admit water clusters; thus, they effectively exclude liquid water[30]. Although beneficial for many applications, MOFs that exclude liquid water cannot find use in aqueous-phase catalysis. Notably, ZIF-8 does not exclude ammonia or hydrogen sulfide and can be degraded by both. Additional contributing factors to the resistance of ZIF-8 to hydrolysis are the comparatively strong bonding between the 2-methylimidazolate linker and the single zinc ion constituting the node, and the effective physical shielding of Zn(II) by four tetrahedrally coordinated 2-methylimidazolate linkers. Shielding and

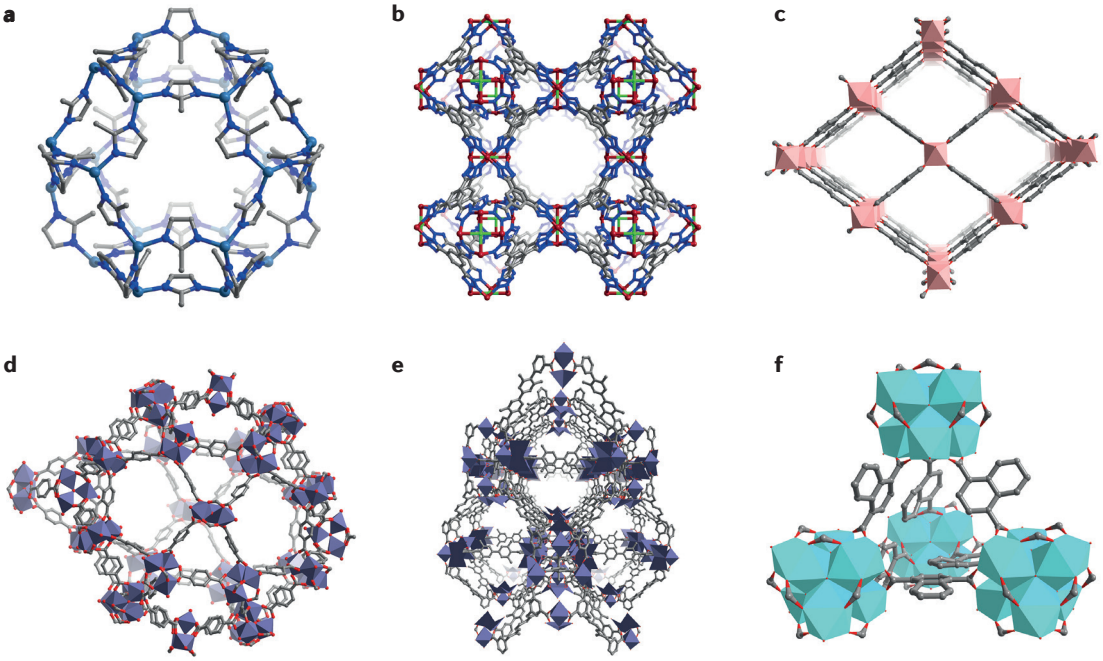

Figure 2 | **Selected sections of representative metal–organic framework materials. a** | ZIF-8. **b** | Cu-BTTri. **c** | MIL-53(Al). **d** | MIL-101(Cr). **e** | PCN-426-Cr(III). **f** | $[(CH_3)_2NH_2]_2$ $[Eu_6(\mu_3\text{-}OH)_8(1,4\text{-}NDC)_6(H_2O)_6]$. Zn, blue-green; N, blue; C, grey; O, red; Cu, brown; Cl, bright green; Al, light pink; Cr, dark blue; Eu, teal. Hydrogen atoms are omitted for clarity. 1,4-NDC, 1,4-naphthalenedicarboxylate; BTTri, 1,3,5-tris(1*H*-1,2,3-triazol-5-yl)benzene; MIL, Materials Institute Lavoisier; PCN, porous coordination network; ZIF, zeolitic imidazolate framework.

bond strength are important factors in stabilizing a large number of MOFs[28,31,68]. For MOFs featuring more open nodes, shielding can often be accomplished with strategically positioned hydrophobic linker substituents such as methyl or trifluoromethyl groups[28,69]. Extended hydrocarbon or fluorinated substituents can contribute further stability by reducing MOF pore volumes and thereby shrinking the size of incorporated water clusters[28].

Relative stabilities of azolate MOFs are related, in part, to the strengths of the metal–nitrogen bonds, which roughly correlate with pK_a values of corresponding molecular azole or azole-containing species. In general, the higher the pK_a for nitrogen deprotonation, the more hydrolytically stable the MOF[70]. An example of an organic acid that forms a robust framework is 1,3,5-tris(1*H*-pyrazol-4-yl)benzene (H_3BTP) for which the pK_a is 19.8. The MOF $Ni_3(BTP)_2$ was characterized by PXRD and post-experiment analysis of the internal surface area, and was found to be stable in boiling aqueous solutions of pH 2–14 for two weeks[70]. In contrast to ZIF-8, this MOF is permeable to liquid water, and each Ni(II) ligates a removable solvent molecule. Thus, the stability of $Ni_3(BTP)_2$ is primarily a consequence of the high strength of the metal–nitrogen bond. Di-, tri- and tetrazoles generally have lower pK_a values, and, as a result, MOFs constructed from their conjugate bases are less chemically stable[71]. However, some tetrazoles (and metal-tetrazolates), owing to their high nitrogen: carbon ratios, are susceptible to detonation by impact or friction; therefore, appropriate experimental precautions must be taken[72].

The examples above are based mainly on divalent metal ions and nitrogen-linkers. Trivalent metals form strong bonds with oxygen-anion-terminated linkers, and examples of such MOF structures are Materials Institute Lavoisier (MIL) compounds (FIG. 2c,d), which have nodes containing multiple Cr(III), Al(III) or Fe(III) ions and carboxylate-terminated linkers[73–77]. These MOFs show excellent stability in water[74,77], and, in addition, related MOFs composed of trivalent lanthanides, for example Eu(III) (FIG. 2e), Tb(III) and Y(III), also demonstrate good stability in water[78–81]. This stability, which in a few cases occurs in solutions up to pH 14, is mainly attributed to the use of short hydrophobic linkers that shield the lanthanide clusters from exposure to water[80,82,83]. Although the majority of porous Al(III)-containing, and especially Cr(III)-containing, MILs are composed of benzene dicarboxylate (BDC) and closely related linkers, there are examples of Al(III) MILs constructed with expanded linkers including biphenyl-4,4′-dicarboxylate (BPDC), 1,3,5-tris(4-carboxyphenyl) benzene (BTB)[84], benzo-tris-thiophene carboxylate (BTTC) and 4,4′,4″-*s*-triazine-2,4,6-triyl-tribenzoate (TATB)[85], which have also been shown to be stable in water. Related to the discussion of MILs, a tetravalent Ti(IV)-MOF, MIL-125, was not only stable in water, but also robust in the presence of acidic gases[86] such as H_2S.

If stronger bonds are incorporated into the framework — for example, between Zr(IV) (or Hf(IV)) and oxyanions — a much greater number and variety of water-stable MOFs become accessible[27,32,33,44,87–100]. In general, the formation of strong bonds leads to the rapid

precipitation of non-porous layered or amorphous materials, but the use of modulators in the synthesis of zirconium- and hafnium-based MOFs has greatly expanded the library of these materials. Modulators are monotopic ligands (for example, acetate, benzoate and formate) that can compete with linkers, thereby slowing the growth of the MOF and enabling the reversal and correction of bonding errors[88]. This correction of 'mistakes' ensures that the process propagates towards the desired, periodic chemical structure. The method is possible because Zr(IV)–O bonds, despite their exceptional strength, are slightly labile, especially under forcing conditions, such as high temperatures and high modulator concentrations. A related idea, termed solvent-assisted linker exchange, is the displacement of a linker within an intact MOF by an alternative linker in solution. This stepwise synthesis strategy can be used to obtain zirconium MOFs that are difficult to synthesize directly[34]. It should be noted that, consistent with their diminished bond lability relative to Zr(IV)–oxyanion, Cr(III)–oxyanion MOFs have proven unresponsive to solvent-assisted linker exchange[34].

Most zirconium-based MOFs feature Zr_6–oxo, hydroxo or aqua clusters as nodes that, in turn, can be 12-, 10-, 8- or 6-connected by di-, tri- or tetratopic carboxylate linkers[32,33,90–92,95–97,99] (FIG. 3). First reported in 2008, the University of Oslo (UiO) compound, UiO-66, which ideally comprises 12-connected zirconium-based nodes and BDCs as linkers, is the archetypal zirconium MOF[27]. Depending on the synthetic conditions used, UiO-type MOFs are often slightly linker-deficient, for example 10- or 11-connected[89,93], with the resulting structural defects accounting for otherwise unexpected properties such as catalytic activity[23,25,101,102]. Occasionally they are also node-deficient, in which an entire Zr_6 or Hf_6 cluster is missing, creating vacancies in the structure[103]. UiO-66 and related compounds are stable in water, with good resistance to moderately acidic or basic solutions[87,94,104]. The incorporation of hydroxo and aqua clusters in the nodes renders these zirconium-based MOFs hydrophilic. Combined with their water stability, this feature points to the potential of zirconium-based MOFs as catalysts for aqueous-phase chemical reactions. In 2010, a series of UiO-66 derivatives containing modified BDC linkers was described[87]. These MOFs were shown by PXRD to be stable to soaking in aqueous acid to pH 1 (or at least to remain crystalline; no post-soaking porosity data were reported). PXRD measurements revealed that an NO_2-functionalized version of the MOF is uniquely stable to soaking in 1 M NaOH (pH = 13.6)[87]. The reasons are unclear, but might reflect differences in the density of structural defects for various versions, rather than substituent electronic effects on zirconium–oxygen (as part of a carboxylate function) bond strength. Indeed, on the basis of the substituent electronic effects discussed above for azolate frameworks, inferior alkaline stability for UiO-66-NO_2 would be expected.

Apart from UiO-66-NO_2, zirconium-based MOFs are typically unstable in highly alkaline solutions. For example, a series of MOFs constructed from Zr_6 nodes and tetratopic porphyrin linkers in various topologies all degraded when soaked in solutions of pH greater than 11 (REF. 29). In this case, degradation probably occurs by hydroxide substitution for carboxylate (linker) oxygen atoms and, as a consequence, strong zirconium–oxygen (linker) bonds are replaced with similarly strong zirconium–oxygen (hydroxide) bonds. Stability towards substitution depends on the magnitude of the activation barrier to substitution as well as on hydroxide concentration.

Various other zirconium MOFs[29,32,90,95] have been found to resist decomposition in aqueous solutions as acidic as pH 1 (FIG. 1). A sulfated analogue of MOF-808 (FIG. 3) was the first that was found to exhibit superacidity and was synthesized by exposing the parent material to aqueous sulfuric acid — a striking demonstration of the acid tolerance of appropriately designed MOFs[95].

In principle, an attractive approach to producing MOFs of even higher acid and base stability is to replace linker carboxylates with phosphonates, because the latter bind more strongly to Zr(IV). Unfortunately, with stronger binding comes decreased lability and a tendency to form either amorphous coordination polymers or non-porous, layered organic or inorganic compounds[105]. Nevertheless, a few well-defined and porous metal–phosphonate (not Zr) MOFs exist[45].

De novo syntheses can produce only limited numbers of high-stability frameworks; however, indirect synthesis methods — in particular, methods involving building-block replacement (both linker and node) — have proven useful for accessing stable MOFs that are difficult or impossible to construct directly[106–108]. MOFs of pillared-paddlewheel-type connectivity are often readily assembled using zinc salts, for example, but not so readily using nickel salts. Nickel(II) is desirable, however, because it forms stronger bonds with both N- and O-terminated linkers, thereby improving MOF resistance to hydrolysis. In one case, using the porous coordination network PCN-426-Mg(II) as a starting material, and recognizing that bond strengths and lability depend not only on the identity of the metal but also on its oxidation state, Mg(II) was displaced with Cr(II) and then oxidized to Cr(III), a highly substitution-inert species, especially when coordinating oxyanions[109]. Indeed, the final form of PCN-426 (FIG. 2f) proved stable in aqueous solutions ranging from pH 0 to 12. However, it should be noted that neither PCN-426-Cr(II) nor PCN-426-Cr(III) is amenable to *de novo* synthesis.

Another approach to slowing or stopping MOF hydrolysis is framework catenation. This involves the assembly of one or more replica frameworks within the void space of the parent framework[28,110]. The stabilizing effects of catenation can arise from blocking the access of water to node–linker bonds, a reduction in the size of the water cluster occupying the voids of the filled MOF, or the favourable dispersion interactions between frameworks.

Thermal stability. Thermal degradation of MOFs is, in most cases, a result of node–linker bond breakage, accompanied or followed by linker combustion. As a consequence, thermal stability is generally related to node–linker bond strength and the number of linkers

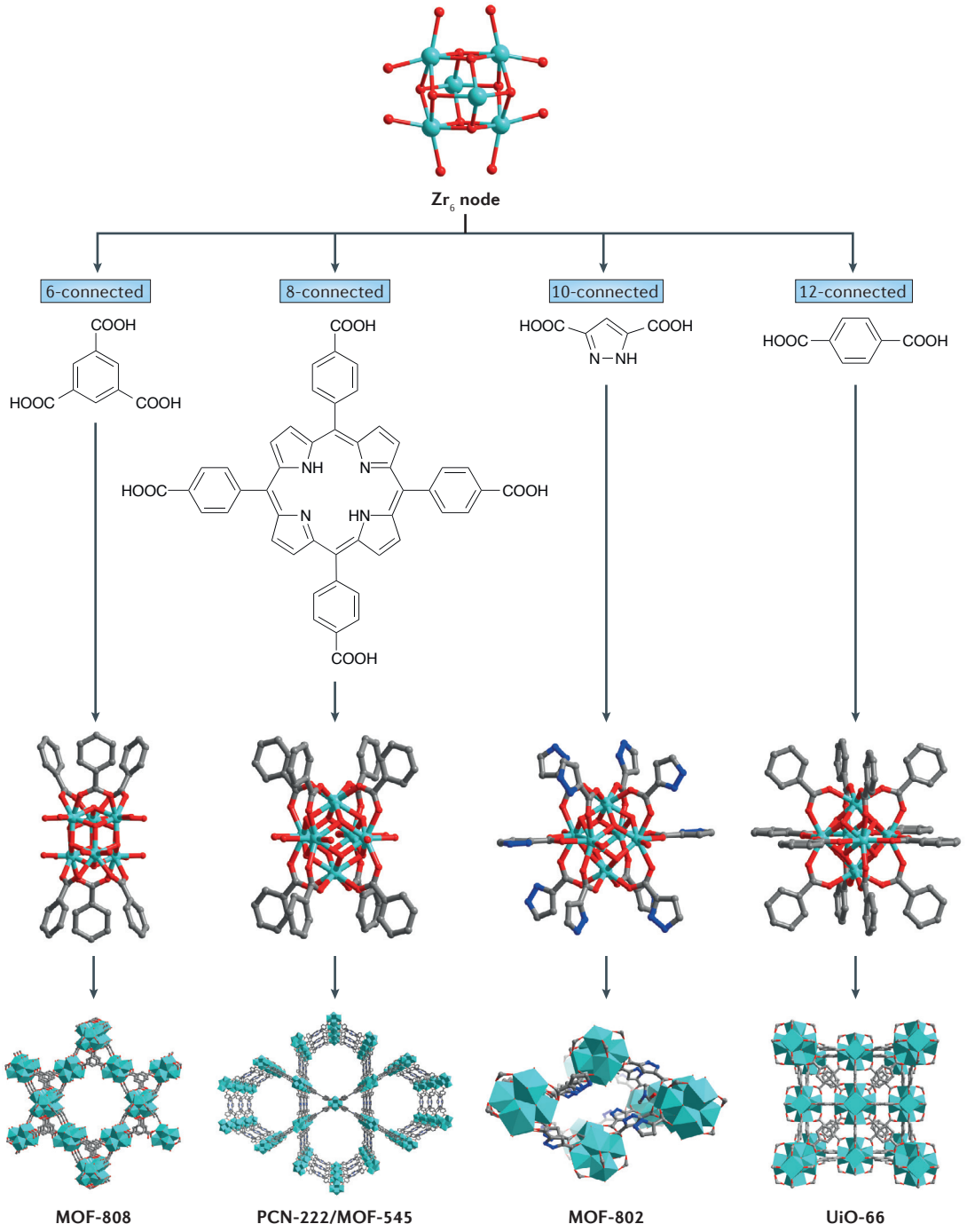

Figure 3 | **Connectivity of Zr_6 nodes in zirconium-based metal–organic frameworks and the associated carboxylate molecules required to link nodes together.** Metal–organic frameworks (MOFs) containing 12-, 10-, 8- and 6-connected Zr_6 nodes have been synthesized. This connectivity refers to the number of linker-associated carboxylates coordinated to each node. Zr, teal; C, grey; O, red; N, blue. Hydrogen atoms are omitted for clarity. PCN, porous coordination network; UiO, University of Oslo.

connected to each node. Thermal degradation may also take the form of MOF amorphization[111], melting[112], node-cluster dehydration[89], or (anaerobic) linker dehydrogenation or graphitization[113,114]. In the linker-graphitization process, the degradation products themselves can be useful materials. Most MOFs incorporate divalent cations (for example, Zn(II), Cu(II), Co(II) and Cd(II)), and carboxylate or N-donating linkers[30,35]. Using equivalent oxyanion-terminated linkers with higher-valency metal centres, such as Ln(III), Al(III), Zr(IV) and Ti(IV), enhances thermal stability by increasing the metal–ligand bond strength[35,99,115]. Another strategy for achieving an increased bond strength and, hence, thermal stability, is changing the composition of linker pendant groups[116].

Framework catenation — more specifically, interpenetration or interweaving of networks — can enhance stability through favourable framework–framework interactions[28]. It has been shown computationally that absolute energies of ZIF polymorphs tend towards lower values as crystal density increases[53]. Consistent with this observation, intentional mechanical stress can engender MOF phase changes towards more stable compounds[117]. However, catenation or other densification strategies can impair some of the intriguing properties of MOFs, such as large pore volumes; therefore, using catenation to impart stability is not always desirable. Nevertheless, for some applications catenation can be beneficial.

Although not yet widely explored, changes in MOF node structure, as a consequence of thermally driven dehydration at temperatures well below that for framework disintegration[89], can have striking effects on the catalytic activity of the MOF structure[24]. Dehydration can occur by the direct loss of aqua ligands at the node or by condensation of hydroxo ligands to yield oxo ligands and molecular water.

Thermogravimetric analysis (TGA) and *in situ* PXRD are both techniques that can be used to gauge the thermal stability of MOFs. TGA is useful for screening, and PXRD yields more detailed information. As a result of the porous nature of MOFs, guest (solvent) molecules are often encapsulated by the framework during synthesis. In a typical TGA experiment under N_2, guests are released between 50 and 100 °C, followed by the loss of coordinated solvent molecules (for example, water, methanol and *N*,*N*′-dimethylformamide) between 100 and 200 °C. The TGA trace then plateaus and ends at the temperature at which framework decomposition and partial volatilization are initiated. Whether the plateau region corresponds to a porous crystalline form of the material is not discernible from TGA measurements alone. Other measurements, such as *in situ* XRD[118], or CO_2 or cryogenic N_2 sorption and desorption after thermal cycling, can be more instructive. In addition, differential scanning calorimetry can be used to reveal phase transitions that escape detection by TGA alone[119]. Performing TGA experiments under air can also be informative for certain applications, because the MOF decomposition process under O_2 can differ from that under N_2. The most thermally inert MOFs — for example, zirconium-based MOF UiO-66 (REF. 31) and others in this family — retain crystallinity and porosity to >500 °C. Thermal stability is often the first type of stability evaluated for new MOFs because high thermal stability is a useful predictor of resistance to other stresses.

Hydrothermal stability. For some applications, such as carbon dioxide capture from flue gas and the catalysis of methanol formation from synthesis gas (H_2 and CO), the instability of MOFs in the presence of moisture at elevated temperatures is a potential limitation[120,121]. MOFs have also been considered as heat storage materials, which function by adsorbing and desorbing vapours (typically, water); hence, hydrothermally stable frameworks are required[122]. Experimentally, hydrothermal stability is assessed by exposing MOFs to steam at various pressures and temperatures, followed by PXRD analysis and porosity or surface-area measurements[123,124]. Hydrothermal stability is critical for certain post-synthetic modification methods such as atomic-layer deposition (ALD) in MOFs (AIM), a process that typically includes exposing the MOF to steam at elevated temperatures. The first reported examples of AIM entailed the exposure of a zirconium-based MOF, Northwestern University NU-1000 (see below), to diethylzinc and trimethylaluminium at 140 and 110 °C, respectively, followed by steam as a coreactant to complete the formation of Zn(II) and Al(III) oxide or hydroxide species on initially hydrated or hydroxylated MOF nodes[99]. For this chemical modification to be successful, the MOFs must have large apertures and channels, as well as hydrothermal stability. In principle, with the right choice of MOF, AIM should be adaptable to the synthesis of node-supported clusters of metal sulfides. For this process, MOFs must be stable to H_2S for exposure times of several minutes and at temperatures of roughly 100 °C. This stability challenge is just beginning to attract substantial attention, albeit in the context of ambient-temperature sulfur capture and removal[48]. Nevertheless, a recent report on cobalt sulfide AIM shows that NU-1000 can be used for this purpose[125].

Among porous carboxylate-based MOFs, those featuring nodes based on multiple Cr(III)[126], Al(III)[127], V(IV)[128], Fe(III)[96] and Zr(IV)[98] tend to show the highest stability to water vapour. By contrast, MOFs containing multiple zinc ions as components of nodes (for example, MOF-5, MOF-177, DUT-30, UMCM-1 and DMOF-1) are generally unstable with respect to extended exposure to high humidity[129]. Quantum mechanical calculations on MOF cluster models and supporting experiments have concluded that the hydrothermal stability of MOFs is highly dependent on node–linker bond strength[120]. For example, the Al–O bond strength in MIL-53 (FIG. 2c) is ~520 kJ mol^{-1}, whereas the strength of the Zn–O bond in MOF-5 is 365 kJ mol^{-1}. More importantly, the activation energy for water displacement of linkers in MIL-53 (180 kJ mol^{-1}) is considerably greater than it is in MOF-5 (50 kJ mol^{-1}). One of the first reported exceptions to the tendency for MOFs based on divalent metal ions and carboxylate-terminated linkers to exhibit poor stability toward water vapour is the porphyrinic Illinois zeolite analogue PIZA-1; the MOF features linear tri-cobalt(II) nodes, greater than 70% porosity and the ability to withstand water vapour repetitively filling and emptying the pores[130]. Another factor that might affect the hydrothermal stability of MOFs is the geometry of the secondary building units (SBUs). A series of zirconium-based MOFs (MIL-140) based on zirconium-oxide-chain SBUs have been shown to have good hydrothermal stability. In addition, these MOFs are more hydrophobic than UiO-66, presumably because the nodes present fewer or no defects and no hydroxyl groups[131].

MOF hydrothermal stability can be enhanced by intermolecular or intramolecular forces, such as internal hydrogen bonding or π stacking[132,133]. Hydrothermal stability can also be improved by introducing hydrophobic

functional groups or perfluorinated linkers[69,134,135], in which the basis for stabilization can come from the inhibition or blockage of sorption of water molecules, the isolation of node–linker bonds from adsorbed water or the restriction of the sizes of water clusters that can form within MOF pores[28]. MOF hydrophobicity can differ markedly in water vapour or liquid water conditions: the latter consists of hydrogen-bonded cohesive clusters of molecules, and the former consists chiefly of isolated molecules. Obviously, single water molecules are smaller than clusters and, thus, are able to permeate materials lacking cluster-sized apertures[28]. Using extensive spectroscopic studies, and drawing on analogies of conventional metal-oxide surfaces, the water-vapour-induced degradation of (non-ZIF) MOFs containing divalent metal ions as nodes has been investigated and considerable mechanistic detail has been revealed[68]. As discussed above, ZIFs as a class comprise excellent examples of hydrophobic MOFs, and many ZIFs are hydrothermally stable, making them reasonable candidates for use in humid conditions[136].

Mechanical stability. MOFs are known for their extraordinary porosity — an attribute that inherently decreases mechanical stability. Therefore, as expected, MOFs are less mechanically stable than zeolites. This instability can manifest itself as phase changes, partial collapse of pores or even amorphization, in response to mechanical loading[53,137–139]. An example is the irreversible amorphization of ZIF-8 (FIG. 2a) at pressures above 0.34 GPa, as shown by *in situ* XRD[140]. In the same study, the concomitant loss in porosity of ZIF-8 was monitored by treating samples with pressures of up to 1.2 GPa (using a hydraulic pellet press) and measuring the nitrogen adsorption and desorption isotherms of the resulting materials. In another method, a simple assessment of survival times for MOF crystallinity during ball milling can be informative. Indeed, such assessment has shown just how damaging the presence of defects (such as missing linkers) can be to MOF mechanical stability[141]. Similar experiments show that solvent-filled MOFs are more mechanically stable than MOFs with empty pores[142].

An under-appreciated source of MOF mechanical degradation is the capillary force exerted when removing strongly associated, pore-filling solvent molecules, especially water. This can easily be mistaken for hydrolytic degradation because the degradation products can appear identical[104]. Notably, many zirconium-based MOFs are susceptible to capillary-force-driven destruction. A way to circumvent this kind of degradation is to exchange the strongly associated solvent with liquid CO_2, and then remove CO_2 under supercritical conditions[9]. These conditions are such that the solvent surface tension is zero and the capillary forces are inherently absent. Another method, suitable for large-channel zirconium-based MOFs, is to attach hydrocarbon or fluorocarbon chains to nodes, thereby eliminating hydrogen-bonding sites between solvent molecules and nodes and, more importantly, decreasing the size of water clusters occupying the channels[28,143].

In the absence of destructive influences, the shear modulus G (susceptibility to distortion in response to a shear force) may be a good predictor of MOF resistance to mechanical degradation[44]. Other properties, such as bulk modulus (resistance to uniform compressibility), hardness and Young's modulus (linear elasticity resistance along one axis), may also be instructive[139]. Hardness and Young's modulus have the virtue of being straightforward to evaluate experimentally by means of nanoindentation measurements. However, apart from the bulk modulus, these properties can be anisotropic. Computational investigations[44,144] have shown that 12-connected (idealized) Hf-UiO-66 has one of the highest shear and bulk moduli of all MOF structures and similar to values typical of zeolites, making it among the most mechanically stable. Experimentally, MIL-140 composed of zirconium oxide chains has shown better mechanical stability than UiO-66; however, the UiO-66 used in this study was not an 'idealized' (defect-free) structure[131]. As computational methods typically neglect defects, calculated moduli often greatly exceed values measured on non-ideal, defect-containing samples. Indeed, such discrepancies can point to the presence of defects in real samples that were previously unrecognized[93,138]. Interestingly, the presence of residual modulators can favourably affect the mechanical stability of missing-linker variants of zirconium-based MOFs, with the magnitude of the stabilization being tunable based on modulator chemical composition[141].

Compared with MOFs based on divalent metals, zirconium-based MOFs generally have superior mechanical stability as a result of the typically high coordination number of the MOF nodes and the high strength of node–linker bonds. MOF geometry is also relevant to mechanical stability or, more specifically, shear-force stability. In the same way that (on a much larger scale) buildings and bridges have more or less stable constructions, some arrangements of linkers and connectors render MOFs more resistant to deformation and destruction than others[44,139,144–146]. Some computational studies show that mechanical stability tends to be enhanced with shorter linkers[44,144].

An important practical development that greatly reduces the mechanical performance requirements for MOFs in applications such as permeation-based chemical separations is the emergence of MOF-containing mixed-matrix membranes, where the second component of the matrix is typically a glassy polymer[147,148].

Finally, albeit outside the scope of this Review, an intriguing subset of MOF structures is made up of those that are intentionally designed to be reversibly flexible and display high mechanical compliance[149–158].

MOF stability in catalytic systems

The idea of using MOFs as heterogeneous catalysts was first articulated 25 years ago[159] and first demonstrated a few years later[160]. Since these initial studies, there have been numerous reports on the use of MOFs in catalysis. The catalytic active site can be several different locations within the structure. It can be incorporated in the MOF linkers[161,162] or nodes[77,163], or encapsulated,

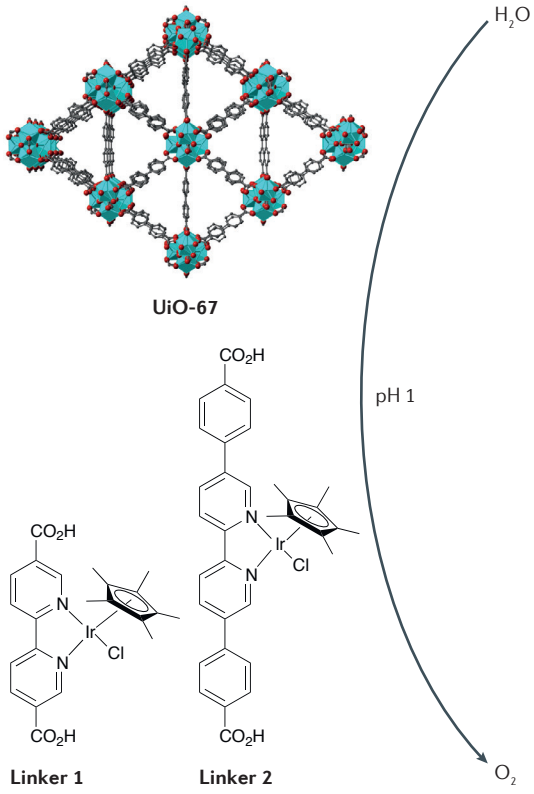

Figure 4 | **Catalytic oxidation of water using Ir-containing derivatives of UiO-67.** The image shows the structure of UiO-67 and Ir-containing linkers 1 and 2 that are utilized for water oxidation catalysis at pH 1. Zr, teal; C, grey; O, red. Hydrogen atoms are omitted for clarity. UiO, University of Oslo.

isolated or stabilized by a MOF[164], or attached to the framework postsynthetically[99,165]. Regardless of the method used to introduce catalytically active sites, the framework must be stable under catalysis conditions. Many industrially relevant catalytic reactions, such as cracking, oligomerization, alkylation and others used for the production of chemical feedstocks and fuels, take place under extreme conditions — some of which clearly exceed those tolerable by even the most stable MOFs. Below we discuss a few examples in which MOFs do indeed measure up.

Solution-phase catalysis. This can constitute acidic, neutral or basic conditions. More specifically, the MOF catalysts need to be able to withstand the conditions appropriate for the chosen reaction. Acetic acid is an important chemical that is produced on an industrial scale from the petrochemical methanol, which, in turn, is made from methane-derived synthesis gas. A potentially attractive alternative to this energy-intensive sequence would be the direct production from methane at modest temperatures. One intriguing example, albeit based on vanadium complexes as homogeneous catalysts with persulfate as an oxygen source, has been reported[166]. An excellent example of the heterogenization of a known homogeneous catalyst is the demonstration of vanadium-based MOF systems (MIL-47 or MOF-48) for the same reaction. These two vanadium-based MOFs have been shown to be stable to repeated 20-hour exposures, catalytically competent and highly selective for conversion of CH_4 and CO to acetic acid, as well as having the advantage of being straightforward to separate from reaction mixtures and recycled[167].

Other examples of MOFs for catalysis under acidic conditions include an analogue of the zirconium-based MOF UiO-67 doped with iridium complexes for water oxidation[161,162] (FIG. 4, linker 1). The UiO-67 MOF doped with iridium is acid-stable and catalytically competent for the four-redox-equivalent oxidation of water to oxygen. With dissolved ceric ammonium nitrate as an oxidant, turnover frequencies per iridium centre are of the order of 0.05 min^{-1}. The catalytic MOF presents apertures of ~7 Å in diameter, which is substantially smaller than the diameter of the ceric ammonium nitrate complex (~11 Å). If the structural defects within the MOF are disregarded, the mismatch between the sizes of the aperture and oxidant size implies that only the outermost iridium complexes can function catalytically[161]. One way of boosting the fraction of participating catalytic sites is to reduce the crystal size of the MOF and thereby increase the fraction of sites residing on the exterior[26]. Another method is to increase the linker length and thereby increase the MOF apertures sufficiently to permit the oxidant to permeate the crystal. By using the latter approach and catalytic linker 2 (FIG. 4), it is possible to increase the turnover frequency of oxygen by a factor of roughly 10 (REF. 162).

There are many examples of persistent, MOF-based catalysis from pH 3 to pH 6. For example, in water at pH 3 the zirconium-based iron porphyrin MOF known as PCN-222(Fe) (also known as MOF-545 (REF. 92) and MMPF-6 (REF. 168)) is competent for the hydrogen-peroxide-driven catalytic oxidation of 3,3,5,5-tetramethylbenzidine[91]. The use of MOFs as catalysts under physiological conditions has also been explored[169,170]; for example, CuBTTri (FIG. 1), which proved stable in phosphate buffer solution at pH 7.4 for 3 days at 37 °C, is catalytic for the release of the biological signalling molecule nitric oxide from *S*-nitrosothiols. Notably, CuBTTri remains catalytic after exposure to fresh citrated whole blood (pH 7.4)[170]. In addition, there are several examples of MOFs as stable catalysts in moderately alkaline environments ($8 < pH < 11$)[21,23–25,171]; an extended example is described below.

Nerve agents such as sarin and soman (also known as GB and GD, respectively) are phosphoester-containing chemical warfare agents[49]. As reports of their use in ongoing conflicts have attained international visibility, attention has turned to their chemical destruction. One strategy for their destruction is hydrolysis (for example, of the phosphorus–fluorine bonds in real agents and the phosphorus–alkoxy bonds in simulants). As a consequence of the strong Lewis acidity of Zr(IV), it was reasoned that zirconium-based MOFs featuring reactant-displaceable aqua ligands might be catalytic for agent or simulant hydrolysis, yet not be

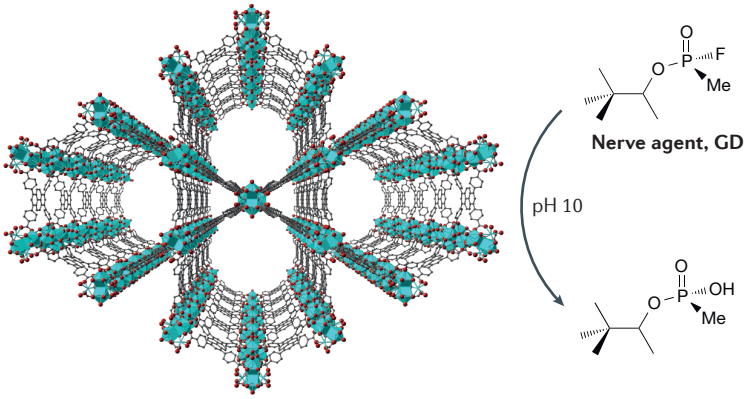

Figure 5 | **Catalytic hydrolysis of the nerve agent soman (known as GD) by NU-1000.** This schematic shows the hydrolysis of the nerve agent GD to *o*-pinacolyl methylphosphonic acid. Zr, teal; C, grey; O, red. Hydrogen atoms are omitted for clarity. NU, Northwestern University.

so strongly interacting that hydrolysis products would inhibit further catalytic activity[21,23–25]. Initial investigations were focused on UiO-66 as a catalyst for hydrolysis of aqueous solutions of paraoxon, a simulant of the nerve agent sarin. It should be noted that catalysis requires the presence of defects: more specifically, aqua and oxo ligands in place of linkers. The observed kinetic behaviour is pseudo-first-order, implying that product inhibition is negligible. With UiO-66, the observed reaction half-life (45 minutes) compares well with the best-performing abiotic catalysts. However, GB and GD function by inhibiting control of pulmonary muscles, resulting in oxygen deprivation and eventually death by asphyxiation. Thus, catalysts that can degrade agents much more rapidly (and that can be administered to people suffering agent exposure) are clearly desirable.

To allow comparisons with literature data, measurements with UiO-66 as a catalyst were made in a buffer solution of pH 10. Post-catalysis characterization, including PXRD measurements, scanning electron microscopy and transmission electron microscopy, showed that UiO-66 remains stable under these reaction conditions[23]. Moreover, there are several synthetic strategies that have been shown to enhance catalytic activity. First, derivatives of UiO-66 and UiO-67 with linker-pendant Brønsted bases were prepared to aid proton transfer and local generation of OH^- (the species that initiates hydrolysis), and these MOFs were shown to perform better than the parent frameworks. Second, nanoparticulate zirconium-based MOFs with larger fractions of exterior-surface-located or easily accessed active sites performed better than the micrometre-sized particles of zirconium-based MOFs that are typically used[26]. Third, NU-1000, a material with much larger apertures, allowing for reactant transport to the MOF interior, and with lower linker-node connectivity than that of UiO-66 or UiO-67, leaving more node coordination sites for catalytic use, showed higher catalytic activity than the UiO-derivatives studied[24]. Finally, MOF-808, with even lower node connectivity (6-connectivity) than that of NU-1000 and thus even more candidate catalytic sites, showed superior hydrolysis activity. Indeed, in the most favourable case (roughly 16:1 simulant:node ratio; catalyst MOF-808) paraoxon hydrolysis is complete within 30 s (REF. 172). A combined experimental and computational study of both node-hydrated and node-dehydrated NU-1000 as a catalyst for the agent GD (*o*-pinacolyl methylphosphonofluoridate; FIG. 5) showed that GD can be degraded with a half-life of just 3 minutes, and established the accurate use of paraoxon as an agent simulant[21]. The study also yielded significant mechanistic insight, showing that hydrolysis occurs by a different pathway than those known for agent-active enzymes. Consistent with the anticipated stability of zirconium-based MOFs in moderately basic aqueous solutions, there was no evidence for catalyst degradation in these studies. Perhaps the most important conclusion is that the synthetic chemistry of water-stable MOFs, especially zirconium-based MOFs, has progressed enough that systematic, hypothesis-driven improvement of MOF catalyst performance has been possible in the past couple of years.

High-temperature catalysis of gas-phase reactions. The use of MOFs for gas-phase catalysis is in an early phase, and most investigations have focused on proof-of-concept reactions such as the oxidation of CO to CO_2. The complexes Co-MOF-5, Cu(5-methylisophthalate)[173], $Cu_5(OH)_2$(5-nitroisophthalate)$_4$ (REF. 174) and $[Ni_8L_{12}]^{20-}$ (H_3L = 4,5-imidazoledicarboxylic acid)[175], as well as MOF-encapsulated nanoparticles such as Au@ZIF-8 (REF. 176) and Au@UiO-66 (REF. 177), have all been found to catalyse this process. Notably, MOFs are often effective at inhibiting nanoparticle sintering, thereby preserving activity that is characteristic of isolated particles[178]. In combination with encapsulated catalysts, the well-defined pores and apertures of pinhole-free MOF shells (more specifically, continuous MOF shells with no defects) can modulate and enhance chemical selectivity, including regioselectivity, both by sterically limiting the access of molecular reactants to nanoparticles and by controlling the orientation of reactants and intermediates. In addition, evidence is emerging for cooperative catalysis based on the strategic positioning of MOF acidic sites on or near metal nanoparticle surfaces[179].

One of the first studies of MOFs for gas-phase carbon dioxide reduction involved depositing metal precursors in the voids of MOF-5 under sublimation-like conditions. The resulting materials were subsequently reduced either by hydrogen treatment at high temperatures or by photolysis under an inert atmosphere (or vacuum) at room temperature to form metal nanoparticles encapsulated by MOF-5 and featuring $Zn_4O(COO)_6$ nodes. Interestingly, one of the materials, Cu@MOF-5, showed activity comparable to Cu/ZnO@MCM-41/48 for methanol production[180], suggesting that Cu@MOF-5 captures the synergistic interactions between copper and ZnO that are crucial for the activity of Cu/ZnO@MCM-41/48 (REF. 120). Unfortunately, the MOF chosen for this early study proved susceptible to degradation by water vapour. Several

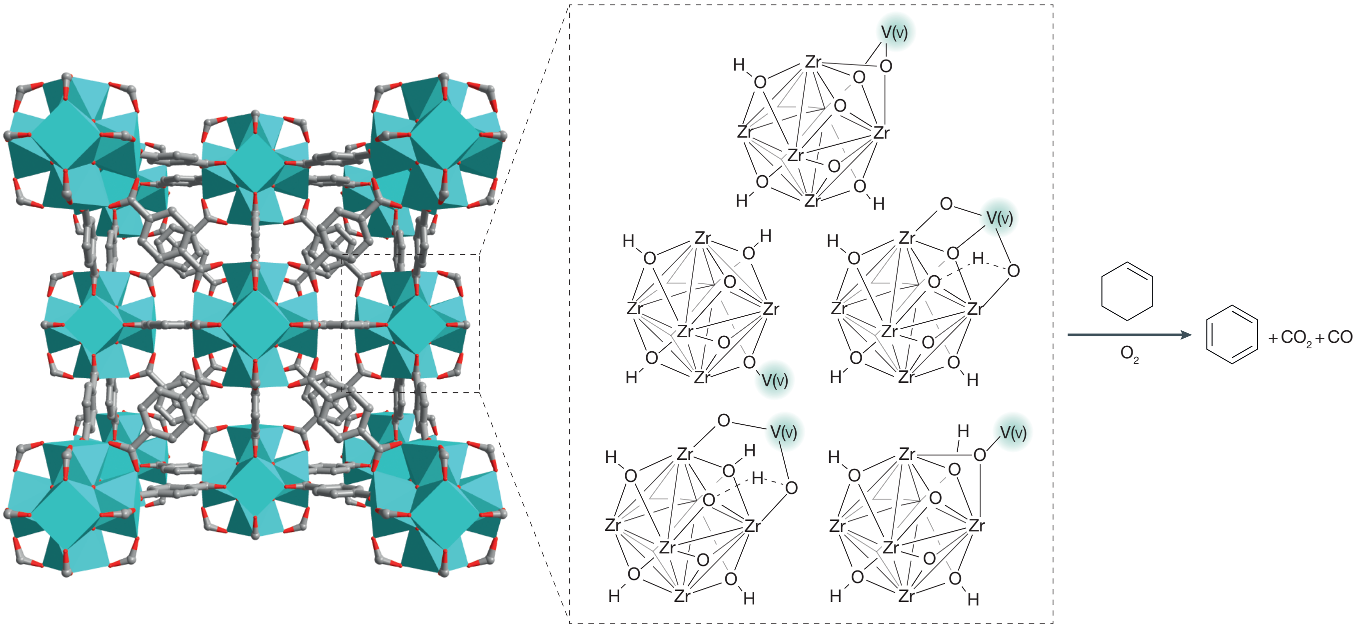

Figure 6 | **Oxidative dehydrogenation of cyclohexene to benzene using V-UiO-66 as a catalyst.** The image shows the structure of UiO-66 indicating all possible V(v) locations on the defects of the node, and a schematic showing the formation of benzene from the oxidative dehydrogenation of cyclohexene. Zr, teal; C, grey; O, red. Hydrogen atoms are omitted for clarity. UiO, University of Oslo.

MOF-based solid acid catalysts with activities that result from a synergetic effect between Brønsted and Lewis acids are efficient catalysts for methanol dehydration[181] or benzylation of aromatic hydrocarbons[182].

Gas-phase catalysis with MOFs has been extended to reactions such as hydrogenation[183], oligomerization of alkenes[184] and dehydrogenation of alkanes[185], which are more typically catalysed by metal or metal-oxide catalysts supported on zeolites, silica, activated carbon or alumina. Reflecting their molecular origins, a virtue of MOFs is the comparative ease with which catalysts can be synthesized in uniform, 'single site' (that is, single metal atom, single metal complex or well-defined cluster[186]) and highly dispersed form. For example, well-isolated Au(III) ions were attached to chelating functionalities appended to the linkers of IRMOF-3 (the NH_2-BDC analogue of MOF-5). This material proved catalytically active for the hydrogenation of 1,3-butadiene, outperforming a model Au@TiO_2 catalyst in terms of both the turnover frequency and selectivity for butene products[187]. A related example is the oligomerization of propene catalysed by Ni-MOF-74, in which the active sites are the coordinatively unsaturated Ni ions present on the nodes[184]. Ni-MOF-74 showed similar activity for propene oligomerization to that of Ni-exchanged MCM-41 (5 bar propene, 180 °C), but with enhanced selectivity for the linear product.

Recently, a MOF with single-site vanadium anchored to otherwise undercoordinated Zr_6 nodes — missing-linker-type defect sites — in UiO-66 has been synthesized and investigated for its catalytic activity in the formation of benzene from the oxidative dehydrogenation of cyclohexene[185] (FIG. 6). At 250 °C, 100% selectivity for benzene was achieved, and at 350 °C roughly 50% selectivity was achieved. These values are significantly higher than those yielded by various Co clusters supported on metal oxides[188]. Of particular note, the crystallinity of V-UiO-66 persisted after heating at 350 °C for 18 hours in the presence of oxygen, highlighting the feasibility of using suitably designed MOFs for gas-phase reactions occurring under comparatively harsh conditions. A conceptually similar study, but with single-site iridium on either UiO-66 or NU-1000 for ethylene hydrogenation or dimerization, has also been described[189]. In view of the potential for complete and atomically precise structural characterization, we believe that the notion of MOFs as stable and uniform supports for single-site catalysts is an especially exciting one, meriting further development.

Future perspectives

Recent developments in the synthesis of MOFs — most notably, building-block-replacement methods, the introduction of modulators and adaptations of post-synthesis modification — make it possible for the motivated materials scientist or engineer to consider 'MOFs by design'. For MOFs to be used as catalysts or catalyst supports, it is important to consider the chemical, thermal and mechanical stabilities of the MOF. Although no single MOF yet embodies all of the following properties, examples now exist of MOFs with some pertinent properties, for example: thermal stability to above 500 °C in an inert atmosphere and at least 350 °C in oxidizing atmospheres; shear and Young's moduli approaching (at least computationally) those of typical zeolites; prolonged stability on immersion in

boiling water; resistance from degradation by steam above 100 °C; and stability in aqueous acid at pH < 0 or aqueous base at pH >14. These features point to emerging and expanding opportunities to obtain well-defined heterogeneous catalysts for elevated-temperature gas-phase reactions and electrochemically or photoelectrochemically driven reactions such as water splitting, hydrogen production and the production of other 'solar fuels' — reactions that all require extreme pH.

It is difficult to envisage MOF structures with stabilities that greatly exceed the thermal, mechanical and chemical stabilities of the most robust existing MOFs. A challenge is to gain routine, rather than exceptional, synthetic access to topologically and chemically diverse MOFs that can persist and function at these stability limits. Among the more specific challenges of probable functional significance are the discovery and implementation of design principles, and the associated chemistry, for the routine synthesis of new MOFs that can tolerate extended exposure, under humid conditions and at elevated temperatures, to corrosive acidic gases. The corresponding applications would be in hydrocarbon separations and heterogeneous catalysis.

The extended mechanical and chemical stabilities of MOFs in thin-film form are also attractive goals. In particular, this includes supported thin films and, more specifically, the persistent and uniform adhesion of the films to their supports, even under the harsh conditions of some catalytic reactions. For electrochemical and electrocatalytic applications of MOF films, it is desirable for the films to be mechanically stable to repetitive ingress and egress of anions and cations, as well as being chemically stable towards the formation of linker-based organic radicals. Stable radicals provide a means for conductivity — involving redox hopping — within MOF films. The conductivity of the MOF film or material is relevant to applications in electrocatalysis.

The systematic passivation of structural defects within MOFs that may otherwise be targeted as weak points for attachment, and hence the degradation of the material, is another approach that could offer more stable structures. For this, it may be that hypothesis-driven computational assessments of ideal and defect-containing versions of both known and not-yet-synthesized materials are important[160].

In summary, MOFs, as a class of porous materials, have moved from the realm of 'usually delicate' and 'usually moisture sensitive' to nearly routinely designable to withstand harsh physical and chemical conditions. This change will no doubt accelerate the exploration and the application of MOFs, in unique ways, to scientifically and technologically significant problems.

1. Abrahams, B. F., Hoskins, B. F., Michail, D. M. & Robson, R. Assembly of porphyrin building blocks into network structures with large channels. *Nature* **369**, 727–729 (1994).
2. Zhou, H.-C., Long, J. R. & Yaghi, O. M. Introduction to metal–organic frameworks. *Chem. Rev.* **112**, 673–674 (2012).
3. Furukawa, H., Cordova, K. E., O'Keeffe, M. & Yaghi, O. M. The chemistry and applications of metal–organic frameworks. *Science* **341**, 1230444 (2013).
4. Horike, S., Shimomura, S. & Kitagawa, S. Soft porous crystals. *Nat. Chem.* **1**, 695–704 (2009).
5. Eddaoudi, M., Sava, D. F., Eubank, J. F., Adil, K. & Guillerm, V. Zeolite-like metal–organic frameworks (ZMOFs): design, synthesis, and properties. *Chem. Soc. Rev.* **44**, 228–249 (2015).
6. Kitagawa, S., Kitaura, R. & Noro, S. Functional porous coordination polymers. *Angew. Chem. Int. Ed. Engl.* **43**, 2334–2375 (2004).
7. Ferey, G. Hybrid porous solids: past, present, future. *Chem. Soc. Rev.* **37**, 191–214 (2008).
8. Foo, M. L., Matsuda, R. & Kitagawa, S. Functional hybrid porous coordination polymers. *Chem. Mater.* **26**, 310–322 (2014).
9. Farha, O. K. & Hupp, J. T. Rational design, synthesis, purification, and activation of metal–organic framework materials. *Acc. Chem. Res.* **43**, 1166–1175 (2010).
10. O'Keeffe, M. & Yaghi, O. M. Deconstructing the crystal structures of metal–organic frameworks and related materials into their underlying nets. *Chem. Rev.* **112**, 675–702 (2012).
11. Farha, O. K. *et al.* Metal–organic framework materials with ultrahigh surface areas: is the sky the limit? *J. Am. Chem. Soc.* **134**, 15016–15021 (2012).
12. Grunker, R. *et al.* A new metal–organic framework with ultra-high surface area. *Chem. Commun.* **50**, 3450–3452 (2014).
13. Furukawa, H. *et al.* Ultrahigh porosity in metal–organic frameworks. *Science* **329**, 424–428 (2010).
14. Furukawa, H. *et al.* Isoreticular expansion of metal–organic frameworks with triangular and square building units and the lowest calculated density for porous crystals. *Inorg. Chem.* **50**, 9147–9152 (2011).
15. Li, J.-R., Kuppler, R. J. & Zhou, H.-C. Selective gas adsorption and separation in metal–organic frameworks. *Chem. Soc. Rev.* **38**, 1477–1504 (2009).
16. Mason, J. A., Veenstra, M. & Long, J. R. Evaluating metal–organic frameworks for natural gas storage. *Chem. Sci.* **5**, 32–51 (2014).
17. Peng, Y. *et al.* Methane storage in metal–organic frameworks: current records, surprise findings, and challenges. *J. Am. Chem. Soc.* **135**, 11887–11894 (2013).
18. Li, J.-R., Sculley, J. & Zhou, H.-C. Metal–organic frameworks for separations. *Chem. Rev.* **112**, 869–932 (2012).
19. Horcajada, P. *et al.* Metal–organic frameworks as efficient materials for drug delivery. *Angew. Chem. Int. Ed. Engl.* **45**, 5974–5978 (2006).
20. Lee, J. *et al.* Metal–organic framework materials as catalysts. *Chem. Soc. Rev.* **38**, 1450–1459 (2009).
21. So, M. C., Wiederrecht, G. P., Mondloch, J. E., Hupp, J. T. & Farha, O. K. Metal–organic framework materials for light-harvesting and energy transfer. *Chem. Commun.* **51**, 3501–3510 (2015).
22. Wang, J.-L., Wang, C. & Lin, W. Metal–organic frameworks for light harvesting and photocatalysis. *ACS Catal.* **2**, 2630–2640 (2012).
23. Katz, M. J. *et al.* Simple and compelling biomimetic metal–organic framework catalyst for the degradation of nerve agent simulants. *Angew. Chem. Int. Ed. Engl.* **53**, 497–501 (2014).
24. Katz, M. J. *et al.* Exploiting parameter space in MOFs: a 20-fold enhancement of phosphate-ester hydrolysis with UiO-66-NH_2. *Chem. Sci.* **6**, 2286–2291 (2015).
25. Nunes, P., Gomes, A. C., Pillinger, M., Gonçalves, I. S. & Abrantes, M. Promotion of phosphoester hydrolysis by the Zr(IV)-based metal–organic framework UiO-67. *Micropor. Mesopor. Mater.* **208**, 21–29 (2015).
26. López-Maya, E. *et al.* Textile/metal–organic-framework composites as self-detoxifying filters for chemical-warfare agents. *Angew. Chem. Int. Ed. Engl.* **54**, 6790–6794 (2015).
27. Cavka, J. H. *et al.* A new zirconium inorganic building brick forming metal–organic frameworks with exceptional stability. *J. Am. Chem. Soc.* **130**, 13850–13851 (2008).
28. Burtch, N. C., Jasuja, H. & Walton, K. S. Water stability and adsorption in metal–organic frameworks. *Chem. Rev.* **114**, 10575–10612 (2014).
29. Bosch, M., Zhang, M. & Zhou, H.-C. Increasing the stability of metal–organic frameworks. *Adv. Chem.* **2014**, 182327 (2014).
30. Park, K. S. *et al.* Exceptional chemical and thermal stability of zeolitic imidazolate frameworks. *Proc. Natl Acad. Sci. USA* **103**, 10186–10191 (2006).
31. Canivet, J., Fateeva, A., Guo, Y., Coasne, B. & Farrusseng, D. Water adsorption in MOFs: fundamentals and applications. *Chem. Soc. Rev.* **43**, 5594–5617 (2014).
32. Bon, V., Senkovska, I., Baburin, I. A. & Kaskel, S. Zr- and Hf-based metal–organic frameworks: tracking down the polymorphism. *Cryst. Growth Des.* **13**, 1231–1237 (2013).
33. Wang, T. C. *et al.* Ultrahigh surface area zirconium MOFs and insights into the applicability of the BET theory. *J. Am. Chem. Soc.* **137**, 3585–3591 (2015).
34. Kim, M., Cahill, J. F., Fei, H., Prather, K. A. & Cohen, S. M. Postsynthetic ligand and cation exchange in robust metal–organic frameworks. *J. Am. Chem. Soc.* **134**, 18082–18088 (2012).
35. Devic, T. & Serre, C. High valence 3*p* and transition metal based MOFs. *Chem. Soc. Rev.* **43**, 6097–6115 (2014).
36. Lee, K., Howe, J. D., Lin, L.-C., Smit, B. & Neaton, J. B. Small-molecule adsorption in open-site metal–organic frameworks: a systematic density functional theory study for rational design. *Chem. Mater.* **27**, 668–678 (2015).
37. Colon, Y. J. & Snurr, R. Q. High-throughput computational screening of metal–organic frameworks. *Chem. Soc. Rev.* **43**, 5735–5749 (2014).
38. Férey, G., Mellot-Draznieks, C., Serre, C. & Millange, F. Crystallized frameworks with giant pores: are there limits to the possible? *Acc. Chem. Res.* **38**, 217–225 (2005).
39. Haldoupis, E., Nair, S. & Sholl, D. S. Pore size analysis of > 250,000 hypothetical zeolites. *Phys. Chem. Chem. Phys.* **13**, 5053–5060 (2011).
40. Zhao, X. *et al.* Selective anion exchange with nanogated isoreticular positive metal–organic frameworks. *Nat. Commun.* **4**, 2344 (2013).
41. Liu, X., Demir, N. K., Wu, Z. & Li, K. Highly water-stable zirconium metal–organic framework UiO-66 membranes supported on alumina hollow fibers for desalination. *J. Am. Chem. Soc.* **137**, 6999–7002 (2015).
42. Henninger, S. K., Habib, H. A. & Janiak, C. MOFs as adsorbents for low temperature heating and cooling applications. *J. Am. Chem. Soc.* **131**, 2776–2777 (2009).

43. Cadiau, A. *et al.* Design of hydrophilic metal–organic framework water adsorbents for heat reallocation. *Adv. Mater.* **27**, 4775–4780 (2015).
44. Wu, H., Yildirim, T. & Zhou, W. Exceptional mechanical stability of highly porous zirconium metal–organic framework UiO-66 and its important implications. *J. Phys. Chem. Lett.* **4**, 925–930 (2013).
45. Ramaswamy, P., Wong, N. E. & Shimizu, G. K. MOFs as proton conductors — challenges and opportunities. *Chem. Soc. Rev.* **43**, 5913–5932 (2014).
46. Sadakiyo, M., Yamada, T. & Kitagawa, H. Rational designs for highly proton-conductive metal–organic frameworks. *J. Am. Chem. Soc.* **131**, 9906–9907 (2009).
47. Horike, S., Umeyama, D. & Kitagawa, S. Ion conductivity and transport by porous coordination polymers and metal–organic frameworks. *Acc. Chem. Res.* **46**, 2376–2384 (2013).
48. Barea, E., Montoro, C. & Navarro, J. A. R. Toxic gas removal — metal–organic frameworks for the capture and degradation of toxic gases and vapours. *Chem. Soc. Rev.* **43**, 5419–5430 (2014).
49. DeCoste, J. B. & Peterson, G. W. Metal–organic frameworks for air purification of toxic chemicals. *Chem. Rev.* **114**, 5695–5727 (2014).
50. Huxford, R. C., Della Rocca, J. & Lin, W. Metal–organic frameworks as potential drug carriers. *Curr. Opin. Chem. Biol.* **14**, 262–268 (2010).
51. Horcajada, P. *et al.* Metal–organic frameworks in biomedicine. *Chem. Rev.* **112**, 1232–1268 (2012).
52. Liédana, N., Galve, A., Rubio, C., Téllez, C. & Coronas, J. CAF@ZIF-8: one-step encapsulation of caffeine in MOF. *ACS Appl. Mater. Interfaces* **4**, 5016–5021 (2012).
53. Tan, J. C. & Cheetham, A. K. Mechanical properties of hybrid inorganic–organic framework materials: establishing fundamental structure-property relationships. *Chem. Soc. Rev.* **40**, 1059–1080 (2011).
54. Abney, C. W. *et al.* Topotactic transformations of metal–organic frameworks to highly porous and stable inorganic sorbents for efficient radionuclide sequestration. *Chem. Mater.* **26**, 5231–5243 (2014).
55. Cunha, D. *et al.* Rationale of drug encapsulation and release from biocompatible porous metal–organic frameworks. *Chem. Mater.* **25**, 2767–2776 (2013).
56. Mouchaham, G. *et al.* A robust infinite zirconium phenolate building unit to enhance the chemical stability of Zr MOFs. *Angew. Chem. Int. Ed. Engl.* **54**, 13297–13301 (2015).
57. Huang, X., Zhang, J. & Chen, X. $[Zn(bim)_2]\cdot(H_2O)_{1.67}$: a metal–organic open-framework with sodalite topology. *Chin. Sci. Bull.* **48**, 1531–1534 (2003).
58. Zhang, J.-P., Zhang, Y.-B., Lin, J.-B. & Chen, X.-M. Metal azolate frameworks: from crystal engineering to functional materials. *Chem. Rev.* **112**, 1001–1033 (2012).
59. Banerjee, R. *et al.* Control of pore size and functionality in isoreticular zeolitic imidazolate frameworks and their carbon dioxide selective capture properties. *J. Am. Chem. Soc.* **131**, 3875–3877 (2009).
60. Banerjee, R. *et al.* High-throughput synthesis of zeolitic imidazolate frameworks and application to CO_2 capture. *Science* **319**, 939–943 (2008).
61. Phan, A. *et al.* Synthesis, structure, and carbon dioxide capture properties of zeolitic imidazolate frameworks. *Acc. Chem. Res.* **43**, 58–67 (2010).
62. Huang, X. C., Lin, Y. Y., Zhang, J. P. & Chen, X. M. Ligand-directed strategy for zeolite-type metal–organic frameworks: zinc(II) imidazolates with unusual zeolitic topologies. *Angew. Chem. Int. Ed. Engl.* **45**, 1557–1559 (2006).
63. Zhang, J. P. & Chen, X. M. Crystal engineering of binary metal imidazolate and triazolate frameworks. *Chem. Commun.* 1689–1699 (2006).
64. Zhang, J. P., Lin, Y. Y., Huang, X. C. & Chen, X. M. Copper(I) 1,2,4-triazolates and related complexes: studies of the solvothermal ligand reactions, network topologies, and photoluminescence properties. *J. Am. Chem. Soc.* **127**, 5495–5506 (2005).
65. Li, J.-R. *et al.* Selective gas adsorption and unique structural topology of a highly stable guest-free zeolite-type MOF material with N-rich chiral open channels. *Chem. Eur. J.* **14**, 2771–2776 (2008).
66. Alkordi, M. H. & Eddaoudi, M. in *Supramolecular Chemistry: From Molecules to Nanomaterials* Vol. 6 (eds Steed, J. W. & Gale, P. A.) 3087–3107 (Wiley, 2012).
67. Liu, Y., Kravtsov, V. C. & Eddaoudi, M. Template-directed assembly of zeolite-like metal–organic frameworks (ZMOFs): a usf-ZMOF with an unprecedented zeolite topology. *Angew. Chem. Int. Ed. Engl.* **47**, 8446–8449 (2008).
68. Tan, K. *et al.* Water interactions in metal–organic frameworks. *CrystEngComm* **17**, 247–260 (2015).
69. Yang, C. *et al.* Fluorous metal–organic frameworks with superior adsorption and hydrophobic properties toward oil spill cleanup and hydrocarbon storage. *J. Am. Chem. Soc.* **133**, 18094–18097 (2011).
70. Colombo, V. *et al.* High thermal and chemical stability in pyrazolate-bridged metal–organic frameworks with exposed metal sites. *Chem. Sci.* **2**, 1311–1319 (2011).
71. Dincă, M., Yu, A. F. & Long, J. R. Microporous metal–organic frameworks incorporating 1,4-benzeneditetrazolate: syntheses, structures, and hydrogen storage properties. *J. Am. Chem. Soc.* **128**, 8904–8913 (2006).
72. Fischer, N., Klapotke, T. M., Scheutzow, S. & Stierstorfer, J. Hydrazinium 5-aminotetrazolate: an insensitive energetic material containing 83.72% nitrogen. *Cent. Eur. J. Energ. Mater.* **5**, 3–18 (2008).
73. Serre, C. *et al.* Very large breathing effect in the first nanoporous chromium(III)-based solids: MIL-53 or $Cr^{III}(OH)\cdot\{O_2C–C_6H_4–CO_2\}\cdot\{HO_2C–C_6H_4–CO_2H\}_x\cdot H_2O_y$. *J. Am. Chem. Soc.* **124**, 13519–13526 (2002).
74. Férey, G. *et al.* A chromium terephthalate-based solid with unusually large pore volumes and surface area. *Science* **309**, 2040–2042 (2005).
75. Loiseau, T. *et al.* MIL-96, a porous aluminum trimesate 3D structure constructed from a hexagonal network of 18-membered rings and μ_3-oxo-centered trinuclear units. *J. Am. Chem. Soc.* **128**, 10223–10230 (2006).
76. Surblé, S. *et al.* Synthesis of MIL-102, a chromium carboxylate metal–organic framework, with gas sorption analysis. *J. Am. Chem. Soc.* **128**, 14889–14896 (2006).
77. Horcajada, P. *et al.* Synthesis and catalytic properties of MIL-100(Fe), an iron(III) carboxylate with large pores. *Chem. Commun.* 2820–2822 (2007).
78. Liang, Y.-T. *et al.* Four super water-stable lanthanide-organic frameworks with active uncoordinated carboxylic and pyridyl groups for selective luminescence sensing of Fe^{3+}. *Dalton Trans.* **44**, 13325–13330 (2015).
79. Surblé, S., Serre, C., Millange, F., Pelle, F. & Férey, G. Synthesis, characterisation and properties of a new three-dimensional yttrium–europium coordination polymer. *Solid State Sci.* **7**, 1074–1082 (2005).
80. Xue, D.-X. *et al.* Tunable rare earth fcu-MOF platform: access to adsorption kinetics driven gas/vapor separations via pore size contraction. *J. Am. Chem. Soc.* **137**, 5034–5040 (2015).
81. Alezi, D. *et al.* Quest for highly connected metal–organic framework platforms: rare-earth polynuclear clusters versatility meets net topology needs. *J. Am. Chem. Soc.* **137**, 5421–5430 (2015).
82. Duan, J. *et al.* High $CO_2/N_2/O_2/CO$ separation in a chemically robust porous coordination polymer with low binding energy. *Chem. Sci.* **5**, 660–666 (2014).
83. Duan, J. *et al.* High CO_2/CH_4 and C2 hydrocarbons/CH_4 selectivity in a chemically robust porous coordination polymer. *Adv. Funct. Mater.* **23**, 3525–3530 (2013).
84. Horcajada, P. *et al.* Extended and functionalized porous iron(III) tri- or dicarboxylates with MIL-100/101 topologies. *Chem. Commun.* **50**, 6872–6874 (2014).
85. Feng, D. *et al.* Stable metal–organic frameworks containing single-molecule traps for enzyme encapsulation. *Nat. Commun.* **6**, 5979 (2015).
86. Vaesen, S. *et al.* A robust amino-functionalized titanium(IV) based MOF for improved separation of acid gases. *Chem. Commun.* **49**, 10082–10084 (2013).
87. Kandiah, M. *et al.* Synthesis and stability of tagged UiO-66Zr-MOFs. *Chem. Mater.* **22**, 6632–6640 (2010).
88. Schaate, A. *et al.* Modulated synthesis of Zr-based metal–organic frameworks: from nano to single crystals. *Chem. Eur. J.* **17**, 6643–6651 (2011).
89. Valenzano, L. *et al.* Disclosing the complex structure of UiO-66 metal–organic framework: a synergic combination of experiment and theory. *Chem. Mater.* **23**, 1700–1718 (2011).
90. Bon, V., Senkovskyy, V., Senkovska, I. & Kaskel, S. Zr(IV) and Hf(IV) based metal–organic frameworks with reo-topology. *Chem. Commun.* **48**, 8407–8409 (2012).
91. Feng, D. *et al.* Zirconium-metalloporphyrin PCN-222: mesoporous metal–organic frameworks with ultrahigh stability as biomimetic catalysts. *Angew. Chem. Int. Ed. Engl.* **51**, 10307–10310 (2012).
92. Morris, W. *et al.* Synthesis, structure, and metalation of two new highly porous zirconium metal–organic frameworks. *Inorg. Chem.* **51**, 6443–6445 (2012).
93. Wu, H. *et al.* Unusual and highly tunable missing-linker defects in zirconium metal–organic framework UiO-66 and their important effects on gas adsorption. *J. Am. Chem. Soc.* **135**, 10525–10532 (2013).
94. Furukawa, H. *et al.* Water adsorption in porous metal–organic frameworks and related materials. *J. Am. Chem. Soc.* **136**, 4369–4381 (2014).
95. Jiang, J. *et al.* Superacidity in sulfated metal–organic framework-808. *J. Am. Chem. Soc.* **136**, 12844–12847 (2014).
96. Liu, T.-F. *et al.* Topology-guided design and syntheses of highly stable mesoporous porphyrinic zirconium metal–organic frameworks with high surface area. *J. Am. Chem. Soc.* **137**, 413–419 (2014).
97. Feng, D. *et al.* A highly stable zeotype mesoporous zirconium metal–organic framework with ultralarge pores. *Angew. Chem. Int. Ed. Engl.* **54**, 149–154 (2015).
98. Kalidindi, S. B. *et al.* Chemical and structural stability of zirconium-based metal–organic frameworks with large three-dimensional pores by linker engineering. *Angew. Chem. Int. Ed. Engl.* **54**, 221–226 (2015).
99. Mondloch, J. E. *et al.* Vapor-phase metalation by atomic layer deposition in a metal–organic framework. *J. Am. Chem. Soc.* **135**, 10294–10297 (2013).
100. Seo, Y. K. *et al.* Energy-efficient dehumidification over hierarchically porous metal–organic frameworks as advanced water adsorbents. *Adv. Mater.* **24**, 806–810 (2012).
101. Shearer, G. C. *et al.* Tuned to perfection: ironing out the defects in metal–organic framework UiO-66. *Chem. Mater.* **26**, 4068–4071 (2014).
102. Vermoortele, F. *et al.* Synthesis modulation as a tool to increase the catalytic activity of metal–organic frameworks: the unique case of UiO-66(Zr). *J. Am. Chem. Soc.* **135**, 11465–11468 (2013).
103. Cliffe, M. J. *et al.* Correlated defect nanoregions in a metal–organic framework. *Nat. Commun.* **5**, 4176 (2014).
104. Mondloch, J. E. *et al.* Are Zr_6-based MOFs water stable? Linker hydrolysis versus capillary-force-driven channel collapse. *Chem. Commun.* **50**, 8944–8946 (2014).
105. Gagnon, K. J., Perry, H. P. & Clearfield, A. Conventional and unconventional metal–organic frameworks based on phosphonate ligands: MOFs and UMOFs. *Chem. Rev.* **112**, 1034–1054 (2012).
106. Deria, P. *et al.* Beyond post-synthesis modification: evolution of metal–organic frameworks via building block replacement. *Chem. Soc. Rev.* **43**, 5896–5912 (2014).
107. Dincă, M. & Long, J. R. High-enthalpy hydrogen adsorption in cation-exchanged variants of the microporous metal–organic framework $Mn_3[(Mn_4Cl)_3(BTT)_8(CH_3OH)_{10}]_2$. *J. Am. Chem. Soc.* **129**, 11172–11176 (2007).
108. Cairns, A. J. *et al.* Supermolecular building blocks (SBBs) and crystal design: 12-connected open frameworks based on a molecular cubohemioctahedron. *J. Am. Chem. Soc.* **130**, 1560–1561 (2008).
109. Liu, T.-F. *et al.* Stepwise synthesis of robust metal–organic frameworks via postsynthetic metathesis and oxidation of metal nodes in a single-crystal to single-crystal transformation. *J. Am. Chem. Soc.* **136**, 7813–7816 (2014).
110. Jasuja, H., Jiao, Y., Burtch, N. C., Huang, Y.-g. & Walton, K. S. Synthesis of cobalt-, nickel-, copper-, and zinc-based, water-stable, pillared metal–organic frameworks. *Langmuir* **30**, 14300–14307 (2014).
111. Bennett, T. D. *et al.* Structure and properties of an amorphous metal–organic framework. *Phys. Rev. Lett.* **104**, 115503 (2010).
112. Umeyama, D., Horike, S., Inukai, M., Itakura, T. & Kitagawa, S. Reversible solid-to-liquid phase transition of coordination polymer crystals. *J. Am. Chem. Soc.* **137**, 864–870 (2015).
113. Sun, J.-K. & Xu, Q. Functional materials derived from open framework templates/precursors: synthesis and applications. *Energy Environ. Sci.* **7**, 2071–2100 (2014).
114. Fujiwara, Y.-i. *et al.* Control of pore distribution of porous carbons derived from Mg^{2+} porous coordination polymers. *Inorg. Chem. Front.* **2**, 473–476 (2015).
115. Fu, Y. H. *et al.* An amine-functionalized titanium metal–organic framework photocatalyst with visible-light-induced activity for CO_2 reduction. *Angew. Chem. Int. Ed. Engl.* **51**, 3364–3367 (2012).
116. Makal, T. A., Wang, X. & Zhou, H.-C. Tuning the moisture and thermal stability of metal–organic frameworks through incorporation of pendant hydrophobic groups. *Cryst. Growth Des.* **13**, 4760–4768 (2013).

117. James, S. L. *et al.* Mechanochemistry: opportunities for new and cleaner synthesis. *Chem. Soc. Rev.* **41**, 413–447 (2012).
118. Chen, J. *et al.* Conversion of cellulose and cellobiose into sorbitol catalyzed by ruthenium supported on a polyoxometalate/metal–organic framework hybrid. *ChemSusChem* **6**, 1545–1555 (2013).
119. Mu, B. & Walton, K. S. Thermal analysis and heat capacity study of metal–organic frameworks. *J. Phys. Chem. C* **115**, 22748–22754 (2011).
120. Low, J. J. *et al.* Virtual high throughput screening confirmed experimentally: porous coordination polymer hydration. *J. Am. Chem. Soc.* **131**, 15834–15842 (2009).
121. Muller, M. *et al.* Loading of MOF-5 with Cu and ZnO nanoparticles by gas-phase infiltration with organometallic precursors: properties of Cu/ZnO@ MOF-5 as catalyst for methanol synthesis. *Chem. Mater.* **20**, 4576–4587 (2008).
122. Henninger, S. K., Jeremias, F., Kummer, H. & Janiak, C. MOFs for use in adsorption heat pump processes. *Eur. J. Inorg. Chem.* **2012**, 2625–2634 (2012).
123. Nugent, P. *et al.* Porous materials with optimal adsorption thermodynamics and kinetics for CO_2 separation. *Nature* **495**, 80–84 (2013).
124. Fracaroli, A. M. *et al.* Metal–organic frameworks with precisely designed interior for carbon dioxide capture in the presence of water. *J. Am. Chem. Soc.* **136**, 8863–8866 (2014).
125. Peters, A. W., Li, Z., Farha, O. K. & Hupp, J. T. Atomically precise growth of catalytically active cobalt sulfide on flat surfaces and within a metal–organic framework via atomic layer deposition. *ACS Nano* **9**, 8484–8490 (2015).
126. Bhattacharjee, S., Chen, C. & Ahn, W.-S. Chromium terephthalate metal–organic framework MIL-101: synthesis, functionalization, and applications for adsorption and catalysis. *RSC Adv.* **4**, 52500–52525 (2014).
127. Gaab, M., Trukhan, N., Maurer, S., Gummaraju, R. & Müller, U. The progression of Al-based metal–organic frameworks — from academic research to industrial production and applications. *Micropor. Mesopor. Mater.* **157**, 131–136 (2012).
128. Kang, I. J., Khan, N. A., Haque, E. & Jhung, S. H. Chemical and thermal stability of isotypic metal–organic frameworks: effect of metal ions. *Chem. Eur. J.* **17**, 6437–6442 (2011).
129. Schoenecker, P. M., Carson, C. G., Jasuja, H., Flemming, C. J. J. & Walton, K. S. Effect of water adsorption on retention of structure and surface area of metal–organic frameworks. *Ind. Eng. Chem. Res.* **51**, 6513–6519 (2012).
130. Kosal, M. E., Chou, J.-H., Wilson, S. R. & Suslick, K. S. A functional zeolite analogue assembled from metalloporphyrins. *Nat. Mater.* **1**, 118–121 (2002).
131. Guillerm, V. *et al.* A series of isoreticular, highly stable, porous zirconium oxide based metal–organic frameworks. *Angew. Chem. Int. Ed. Engl.* **51**, 9267–9271 (2012).
132. ul Qadir, N., Said, S. A. M. & Bahaidarah, H. M. Structural stability of metal organic frameworks in aqueous media — controlling factors and methods to improve hydrostability and hydrothermal cyclic stability. *Micropor. Mesopor. Mater.* **201**, 61–90 (2015).
133. Li, W. *et al.* Mechanical tunability via hydrogen bonding in metal–organic frameworks with the perovskite architecture. *J. Am. Chem. Soc.* **136**, 7801–7804 (2014).
134. Yang, J., Grzech, A., Mulder, F. M. & Dingemans, T. J. Methyl modified MOF-5: a water stable hydrogen storage material. *Chem. Commun.* **47**, 5244–5246 (2011).
135. Serre, C. Superhydrophobicity in highly fluorinated porous metal–organic frameworks. *Angew. Chem. Int. Ed. Engl.* **51**, 6048–6050 (2012).
136. Nguyen, N. T. *et al.* Selective capture of carbon dioxide under humid conditions by hydrophobic chabazite-type zeolitic imidazolate frameworks. *Angew. Chem. Int. Ed. Engl.* **53**, 10645–10648 (2014).
137. Katsenis, A. D. *et al. In situ* X-ray diffraction monitoring of a mechanochemical reaction reveals a unique topology metal–organic framework. *Nat. Commun.* **6**, 6662 (2015).
138. Coudert, F.-X. Responsive metal–organic frameworks and framework materials: under pressure, taking the heat, in the spotlight, with friends. *Chem. Mater.* **27**, 1905–1916 (2015).
139. Li, W., Henke, S. & Cheetham, A. K. Research update: mechanical properties of metal–organic frameworks — influence of structure and chemical bonding. *APL Mater.* **2**, 123902 (2014).
140. Chapman, K. W., Halder, G. J. & Chupas, P. J. Pressure-induced amorphization and porosity modification in a metal–organic framework. *J. Am. Chem. Soc.* **131**, 17546–17547 (2009).
141. Van de Voorde, B. *et al.* Improving the mechanical stability of zirconium-based metal–organic frameworks by incorporation of acidic modulators. *J. Mater. Chem. A* **3**, 1737–1742 (2015).
142. Bennett, T. D., Sotelo, J., Tan, J.-C. & Moggach, S. A. Mechanical properties of zeolitic metal–organic frameworks: mechanically flexible topologies and stabilization against structural collapse. *CrystEngComm* **17**, 286–289 (2015).
143. Deria, P., Chung, Y. G., Snurr, R. Q., Hupp, J. T. & Farha, O. K. Water stabilization of Zr_6-based metal–organic frameworks via solvent-assisted ligand incorporation. *Chem. Sci.* **6**, 5172–5176 (2015).
144. Kuc, A., Enyashin, A. & Seifert, G. Metal–organic frameworks: structural, energetic, electronic, and mechanical properties. *J. Phys. Chem. B* **111**, 8179–8186 (2007).
145. Sarkisov, L., Martin, R. L., Haranczyk, M. & Smit, B. On the flexibility of metal–organic frameworks. *J. Am. Chem. Soc.* **136**, 2228–2231 (2014).
146. Tan, J. C., Bennett, T. D. & Cheetham, A. K. Chemical structure, network topology, and porosity effects on the mechanical properties of zeolitic imidazolate frameworks. *Proc. Natl Acad. Sci. USA* **107**, 9938–9943 (2010).
147. Adams, R., Carson, C., Ward, J., Tannenbaum, R. & Koros, W. Metal–organic framework mixed matrix membranes for gas separations. *Micropor. Mesopor. Mater.* **131**, 13–20 (2010).
148. Zornoza, B., Tellez, C., Coronas, J., Gascon, J. & Kapteijn, F. Metal–organic framework based mixed matrix membranes: an increasingly important field of research with a large application potential. *Micropor. Mesopor. Mater.* **166**, 67–78 (2013).
149. Ortiz, A. U., Boutin, A., Fuchs, A. H. & Coudert, F.-X. Metal–organic frameworks with wine-rack motif: what determines their flexibility and elastic properties? *J. Chem. Phys.* **138**, 174703 (2013).
150. Loiseau, T. *et al.* A rationale for the large breathing of the porous aluminum terephthalate (MIL-53) upon hydration. *Chem. Eur. J.* **10**, 1373–1382 (2004).
151. Millange, F., Serre, C., Guillou, N., Ferey, G. & Walton, R. I. Structural effects of solvents on the breathing of metal–organic frameworks: an *in situ* diffraction study. *Angew. Chem. Int. Ed. Engl.* **47**, 4100–4105 (2008).
152. Kitagawa, S. & Uemura, K. Dynamic porous properties of coordination polymers inspired by hydrogen bonds. *Chem. Soc. Rev.* **34**, 109–119 (2005).
153. Serre, C. *et al.* Role of solvent–host interactions that lead to very large swelling of hybrid frameworks. *Science* **315**, 1828–1831 (2007).
154. Zornoza, B. *et al.* Functionalized flexible MOFs as fillers in mixed matrix membranes for highly selective separation of CO_2 from CH_4 at elevated pressures. *Chem. Commun.* **47**, 9522–9524 (2011).
155. Llewellyn, P. L. *et al.* Complex adsorption of short linear alkanes in the flexible metal–organic-framework MIL-53(Fe). *J. Am. Chem. Soc.* **131**, 13002–13008 (2009).
156. Horcajada, P. *et al.* How linker's modification controls swelling properties of highly flexible iron(III) dicarboxylates MIL-88. *J. Am. Chem. Soc.* **133**, 17839–17847 (2011).
157. Millange, F. *et al.* Selective sorption of organic molecules by the flexible porous hybrid metal–organic framework MIL-53(Fe) controlled by various host–guest interactions. *Chem. Mater.* **22**, 4237–4245 (2010).
158. Serre, C. *et al.* An explanation for the very large breathing effect of a metal–organic framework during CO_2 adsorption. *Adv. Mater.* **19**, 2246–2251 (2007).
159. Hoskins, B. F. & Robson, R. Design and construction of a new class of scaffolding-like materials comprising infinite polymeric frameworks of 3D-linked molecular rods. A reappraisal of the zinc cyanide and cadmium cyanide structures and the synthesis and structure of the diamond-related frameworks $[N(CH_3)_4][Cu^{I}Zn^{II}(CN)_4]$ and $Cu^{I}[4,4',4'',4'''$-tetracyanotetraphenylmethane$]BF_4.xC_6H_5NO_2$. *J. Am. Chem. Soc.* **112**, 1546–1554 (1990).
160. Fujita, M., Kwon, Y. J., Washizu, S. & Ogura, K. Preparation, clathration ability, and catalysis of a two-dimensional square network material composed of cadmium(II) and 4,4′-bipyridine. *J. Am. Chem. Soc.* **116**, 1151–1152 (1994).
161. Wang, C., Xie, Z., deKrafft, K. E. & Lin, W. Doping metal–organic frameworks for water oxidation, carbon dioxide reduction, and organic photocatalysis. *J. Am. Chem. Soc.* **133**, 13445–13454 (2011).
162. Wang, C., Wang, J.-L. & Lin, W. Elucidating molecular iridium water oxidation catalysts using metal–organic frameworks: a comprehensive structural, catalytic, spectroscopic, and kinetic study. *J. Am. Chem. Soc.* **134**, 19895–19908 (2012).
163. Schlichte, K., Kratzke, T. & Kaskel, S. Improved synthesis, thermal stability and catalytic properties of the metal–organic framework compound $Cu_3(BTC)_2$. *Micropor. Mesopor. Mater.* **73**, 81–88 (2004).
164. Alkordi, M. H., Liu, Y., Larsen, R. W., Eubank, J. F. & Eddaoudi, M. Zeolite-like metal–organic frameworks as platforms for applications: on metalloporphyrin-based catalysts. *J. Am. Chem. Soc.* **130**, 12639–12641 (2008).
165. Canivet, J., Aguado, S., Schuurman, Y. & Farrusseng, D. MOF-supported selective ethylene dimerization single-site catalysts through one-pot postsynthetic modification. *J. Am. Chem. Soc.* **135**, 4195–4198 (2013).
166. Kirillova, M. V. *et al.* Direct and remarkably efficient conversion of methane into acetic acid catalyzed by amavadine and related vanadium complexes. A synthetic and a theoretical DFT mechanistic study. *J. Am. Chem. Soc.* **129**, 10531–10545 (2007).
167. Phan, A., Czaja, A. U., Gándara, F., Knobler, C. B. & Yaghi, O. M. Metal–organic frameworks of vanadium as catalysts for conversion of methane to acetic acid. *Inorg. Chem.* **50**, 7388–7390 (2011).
168. Gao, W.-Y., Chrzanowski, M. & Ma, S. Metal–metalloporphyrin frameworks: a resurging class of functional materials. *Chem. Soc. Rev.* **43**, 5841–5866 (2014).
169. Harding, J. L. & Reynolds, M. M. Metal–organic frameworks as nitric oxide catalysts. *J. Am. Chem. Soc.* **134**, 3330–3333 (2012).
170. Harding, J. L., Metz, J. M. & Reynolds, M. M. A. Tunable, stable and bioactive MOF catalyst for generating a localized therapeutic from endogenous sources. *Adv. Funct. Mater.* **24**, 7503–7509 (2014).
171. Yuan, B., Pan, Y., Li, Y., Yin, B. & Jiang, H. A. Highly active heterogeneous palladium catalyst for the Suzuki–Miyaura and Ullmann coupling reactions of aryl chlorides in aqueous media. *Angew. Chem. Int. Ed. Engl.* **49**, 4054–4058 (2010).
172. Li, P. *et al.* Synthesis of nanocrystals of Zr-based metal–organic frameworks with csq-net: significant enhancement in the degradation of a nerve agent simulant. *Chem. Commun.* **51**, 10925–10928 (2015).
173. Zou, R. Q., Sakurai, H., Han, S., Zhong, R. Q. & Xu, Q. Probing the Lewis acid sites and CO catalytic oxidation activity of the porous metal–organic polymer [Cu(5-methylisophthalate)]. *J. Am. Chem. Soc.* **129**, 8402–8403 (2007).
174. Zhao, Y. *et al.* CO catalytic oxidation by a metal–organic framework containing high density of reactive copper sites. *Chem. Commun.* **47**, 6377–6379 (2011).
175. Zou, R. Q., Sakurai, H. & Xu, Q. Preparation, adsorption properties, and catalytic activity of 3D porous metal–organic frameworks composed of cubic building blocks and alkali-metal ions. *Angew. Chem. Int. Ed. Engl.* **45**, 2542–2546 (2006).
176. Jiang, H. L. *et al.* Au@ZIF-8: CO oxidation over gold nanoparticles deposited to metal–organic framework. *J. Am. Chem. Soc.* **131**, 11302–11303 (2009).
177. Wu, R. *et al.* Highly dispersed Au nanoparticles immobilized on Zr-based metal–organic frameworks as heterostructured catalyst for CO oxidation. *J. Mater. Chem. A* **1**, 14294–14299 (2013).
178. Hu, P., Morabito, J. V. & Tsung, C.-K. Core–shell catalysts of metal nanoparticle core and metal–organic framework shell. *ACS Catal.* **4**, 4409–4419 (2014).
179. Choi, K. M., Na, K., Somorjai, G. A. & Yaghi, O. M. Chemical environment control and enhanced catalytic performance of platinum nanoparticles embedded in nanocrystalline metal–organic frameworks. *J. Am. Chem. Soc.* **137**, 7810–7816 (2015).

180. Hermes, S. *et al.* Metal@MOF: loading of highly porous coordination polymers host lattices by metal organic chemical vapor deposition. *Angew. Chem. Int. Ed. Engl.* **44**, 6237–6241 (2005).
181. Liang, D.-D., Liu, S.-X., Ma, F.-J., Wei, F. & Chen, Y.-G. A. Crystalline catalyst based on a porous metal–organic framework and 12-tungstosilicic acid: particle size control by hydrothermal synthesis for the formation of dimethyl ether. *Adv. Synth. Catal.* **353**, 733–742 (2011).
182. Li, B. *et al.* Metal–organic framework based upon the synergy of a Brønsted acid framework and Lewis acid centers as a highly efficient heterogeneous catalyst for fixed-bed reactions. *J. Am. Chem. Soc.* **137**, 4243–4248 (2015).
183. Henschel, A., Gedrich, K., Kraehnert, R. & Kaskel, S. Catalytic properties of MIL-101. *Chem. Commun.* 4192–4194 (2008).
184. Mlinar, A. N. *et al.* Selective propene oligomerization with nickel(II)-based metal–organic frameworks. *ACS Catal.* **4**, 717–721 (2014).
185. Nguyen, H. G. T. *et al.* Vanadium-node-functionalized UiO-66: a thermally stable MOF-supported catalyst for the gas-phase oxidative dehydrogenation of cyclohexene. *ACS Catal.* **4**, 2496–2500 (2014).
186. Thomas, J. M. The concept, reality and utility of single-site heterogeneous catalysts (SSHCs). *Phys. Chem. Chem. Phys.* **16**, 7647–7661 (2014).
187. Zhang, X., Llabrés i Xamena, F. X. & Corma, A. Gold(III) — metal–organic framework bridges the gap between homogeneous and heterogeneous gold catalysts. *J. Catal.* **265**, 155–160 (2009).
188. Lee, S. *et al.* Oxidative dehydrogenation of cyclohexene on size selected subnanometer cobalt clusters: improved catalytic performance via evolution of cluster-assembled nanostructures. *Phys. Chem. Chem. Phys.* **14**, 9336–9342 (2012).
189. Yang, D. *et al.* Metal–organic framework nodes as nearly ideal supports for molecular catalysts: NU-1000- and UiO-66-supported iridium complexes. *J. Am. Chem. Soc.* **137**, 7391–7396 (2015).

Acknowledgements
The authors acknowledge the US Defense Threat Reduction Agency (grant HDTRA10-1-0023; nerve agents), the Institute of Catalysis for Energy Processes at Northwestern University (V-AIM catalytic chemistry), the DOE Separations and Analysis program (MOF synthesis methods), and the Inorganometallic Catalyst Design Center, an Energy Frontier Research Center, funded by the US Department of Energy, Office of Science, Basic Energy Sciences (awards DE FG02-03ER15457, DE-FG02-08ER15967 and DE-SC0012702, respectively) for support.

Competing interests statement
The authors declare no competing interests.